



# *Inverse analysis of the nonlinear response of laterally loaded pile*

*Αντίστροφη ανάλυση της μη γραμμικής  
απόκρισης πασσάλου σε εγκάρσια φόρτιση*

by

Konstantina S.Zolota

Diploma thesis supervised by:

**N. Gerolymos**

Assistant Professor N.T.U.A

της

Κωνσταντίνας Σ. Ζολώτα

Διπλωματική εργασία υπό επίβλεψη:

**Ν.Γερόλυμου**

Επίκουρου Καθηγητή Ε.Μ.Π.

in the  
Geotechnical Department  
School of Civil Engineering  
**NATIONAL TECHNICAL  
UNIVERSITY OF ATHENS**

στον  
Τομέα Γεωτεχνικής  
Σχολή Πολιτικών Μηχανικών  
**ΕΘΝΙΚΟ ΜΕΤΣΟΒΙΟ  
ΠΟΛΥΤΕΧΝΕΙΟ**

Athens, March 2015

Αθήνα, Μάρτιος 2015



NATIONAL TECHNICAL UNIVERSITY OF ATHENS

## *Abstract*

School of Civil Engineering  
Geotechnical Department

### *Inverse analysis of the nonlinear response of laterally loaded pile*

by Konstantina S.Zolota

Aim of thesis is the calculation of soil parameters, required for designing pile foundation under lateral load, with speed and acceptable geotechnical accuracy, utilizing the respective incremental static in-situ load test.

Towards this achievement, algorithm was designed, which, given the pile's response, calibrates the soil parameters, converging the reproduced response into the given, by inverse analysis. This algorithm is based on the phenomenological Winkler-type constitutive model BWGG, that considers the inelastic behavior of both soil and pile. The model was reformulated with Implicit Finite Difference equations, for the purpose of compatibility with the optimization techniques.

The technical adequacy of the algorithm was verified using as input source, the feedback results. The physical accuracy was validated by the satisfactory convergence of calculated response into the results of finite element analysis, monotonic static load test, with the soil described by the constitutive model Hardening Soil.

**Keywords:** pile, lateral load, inverse analysis, calibration of soil parameters, BWGG, soil and pile inelasticity, algorithm design



## ΕΘΝΙΚΟ ΜΕΤΣΟΒΙΟ ΠΟΛΥΤΕΧΝΕΙΟ

# Περίληψη

Σχολή Πολιτικών Μηχανικών

Τομέας Γεωτεχνικής

## Αντίστροφη ανάλυση της μη-γραμμικής απόκρισης πασσάλου σε εγκάρσια φόρτιση

της Κωνσταντίνας Σ. Ζολώτα

Στόχος της εργασίας αποτελεί ο υπολογισμός των εδαφικών παράμετρων, απαραίτητων για τον σχεδιασμό θεμελίωσης εγκαρσίων φορτιζομένου πασσάλου, με ταχύτητα και ικανοποιητική γεωτεχνική ακρίβεια, αξιοποιώντας την αντίστοιχη δοκιμαστική επιτόπια στατική επαυξητική φόρτιση.

Για την επίτευξή του, σχεδιάστηκε αλγόριθμος, ο οποίος, δεδομένης της απόκρισης του πασσάλου, βαθμονομεί τις εδαφικές παραμέτρους, συγχλίνοντας την αναπαραγμένη απόκριση στην δεδομένη, με αντίστροφη ανάλυση. Αυτός ο αλγόριθμος βασίζεται στο φαινομενολογικό ελατηριωτό καταστατικό προσομοίωμα BWGG, που θεωρεί ανελαστική τη συμπεριφορά εδάφους και πασσάλου. Το προσομοίωμα επαναδιατυπώθηκε με εξισώσεις Πεπερασμένων Διαφορών Έμμεσης μορφής, για λόγους συμβατότητας με τις τεχνικές βελτιστοποίησης.

Η τεχνική αρτιότητα του αλγορίθμου επαληθεύεται χρησιμοποιώντας, ως πηγή δεδομένων, τα αποτελέσματα ανατροφοδότησης. Η φυσική ορθότητά του επικυρώθηκε από την ικανοποιητική σύγκλιση των υπολογισμένων καμπυλών απόκρισης στα αποτελέσματα ανάλυσης πεπερασμένων στοιχείων, μονοτονικής στατικής φόρτισης, με έδαφος που περιγράφεται από το καταστατικό προσομοίωμα Hardening Soil.

**Λέξεις Κλειδιά:** πάσσαλος, εγκάρσια φόρτιση, αντίστροφη ανάλυση, βαθμονόμηση εδαφικών παράμετρων, BWGG, ανελαστικότητα εδάφους και πασσάλου, σχεδιασμός αλγορίθμου



## *Acknowledgements*

First and foremost, I would like to express my sincere gratitude to my supervisor, *Dr Nikos Gerolymos*, for his continuous support, patience and motivation whilst creative freedom was granted. His knowledge and multiple-perspective thinking were enlightening, making this cooperation an honor for me.

Besides my supervisor, I wish to thank the rest of my thesis committee: *Professor G. Gazetas* and *Dr V. Georgiannou*, Associate Professor, for their approval, the insightful comments and their encouragement.

As far as bibliography is concerned, *A. Platis*, *A. Kampitsis*, *A. Antoniou* and *Y. Athanasiou*'s contribution should be acknowledged.

Furthermore, I would like to express my appreciation to the National Technical University of Athens's community overall. Without the access in services of Virtual Private Networks(VPN) and Cloud Computing, powered by the Network Management and Computer Center, respectively, this thesis would not have been possible.

Appreciation is ,also, absolute to the open-source community. Their software were extensively used all through this project.

Last but not least, I am indebted to my beloved people: family and friends, for their support throughout writing this thesis and in life generally. I thank, additionally, the youngest members of this group, nieces and nephews, who learn me to take pleasure in simplicity.



# Contents

<b>Abstract</b>	<b>iii</b>
<b>Περιληψη</b>	<b>v</b>
<b>Acknowledgements</b>	<b>vii</b>
<b>List of Figures</b>	<b>xi</b>
<b>List of Tables</b>	<b>xiii</b>
<b>1 Introduction</b>	<b>1</b>
<b>2 Algorithm Design</b>	<b>3</b>
2.1 Forward Analysis Algorithm . . . . .	3
2.2 Inverse Analysis Algorithm . . . . .	11
2.3 Assumptions, Delimitations and Limitations . . . . .	13
<b>3 Algorithm Evaluation</b>	<b>17</b>
3.1 Verification . . . . .	17
3.1.1 Input data creation . . . . .	17
3.1.2 Inverse analysis . . . . .	19
3.1.3 Output assessment . . . . .	19
3.2 Validation . . . . .	22
3.2.1 Input data creation . . . . .	22
3.2.2 Inverse analysis . . . . .	26
3.2.3 Output assessment . . . . .	26
<b>4 Conclusions</b>	<b>31</b>
<b>A Inverse Analysis Algorithm: Matlab Code</b>	<b>33</b>
A.1 Guidance on input format . . . . .	33
A.2 Script: main1PL.m . . . . .	35
A.3 Function: fun1PL.m . . . . .	37
A.4 Function: fun2PL.m . . . . .	44

---

<b>B Finite Elements 3D analysis</b>	<b>53</b>
B.1 Input used in Validation Case . . . . .	53
B.1.1 P-y curve . . . . .	53
B.1.2 Displacement's distribution . . . . .	54
B.2 PLAXIS Report . . . . .	55
B.3 Additional output figures . . . . .	69
<b>Bibliography</b>	<b>73</b>

# List of Figures

2.1.1 Laterally loaded pile problem . . . . .	4
2.1.2 Effect of the “n ” parameter on the p-y curve . . . . .	9
2.1.3 Effect of “a” parameter on the p-y curve . . . . .	9
2.1.4 Effect of the“ b”,“g” parameters on the p-y curve . . . . .	9
2.1.5 Forward analysis flowchart . . . . .	10
2.2.1 Optimization function “fminsearch” . . . . .	11
2.2.2 Inverse analysis flowchart . . . . .	12
2.3.1 Winkler-type nonlinear soil model . . . . .	15
2.3.2 Gapping effect . . . . .	15
2.3.3 Cyclic strength degradation . . . . .	16
2.3.4 Pile’s cross-sectional shape . . . . .	16
3.1.1 Verification case: Dialog box gathering input . . . . .	19
3.1.2 Verification case: optimum $k_{elastic}$ . . . . .	20
3.1.3 Verification case: optima $n, P_y, m$ . . . . .	21
3.2.1 3D Finite Element Analysis: Plastic points . . . . .	23
3.2.2 3D Finite Element Analysis: Material elements . . . . .	24
3.2.3 Broms method: single, free-head, piles laterally loaded in cohesionless soil	24
3.2.4 M-N failure envelope of the reinforced concrete pile . . . . .	25
3.2.5 Validation case: Dialog box gathering input . . . . .	27
3.2.6 Validation case: optimum $k_{elastic}$ . . . . .	28
3.2.7 Validation case: optima $n, P_y, m$ . . . . .	29
B.3.1 Total Displacements, $u$ . . . . .	69
B.3.2 Displacement $u_x$ . . . . .	70
B.3.3 Incremental deviatoric strain $\Delta\gamma_s$ . . . . .	71



# List of Tables

3.1.1 Forward Analysis Input . . . . .	18
3.1.2 Verification Case Input . . . . .	18
3.1.3 Verification Case Output . . . . .	18
3.2.1 3D Finite Elements Analysis Input . . . . .	25
3.2.2 Validation Case Output . . . . .	26
3.2.3 Validation Case Input . . . . .	27



*To my goddaughter,  
little yet brave*  
 $\Sigma\tau\rho\alpha\tau\omega\nu\acute{\kappa}\eta$



# Chapter 1

## Introduction

“πάντα ρεῖ, πάντα χωρεῖ καὶ οὐδὲν μένει”

(i.e. there is nothing permanent except change, free translation)

*Heraclitus*, (4th century)

“ce que nous connaissons est peu de chose; ce que nous ignorons est immense”

(i.e. what we know is little; what we do ignore is immense)

*Pierre-Simon Laplace*, (1827)

Fluidity and uncertainty in soil behaviour, in the theories that describe it and in the choice of their parameters, are granted in geotechnical engineering. Thus, inverse analysis of in-situ tests, which calibrates soil constitutive models' parameters and verifies their results, is critical.

In this thesis, *aim* is the optimization of the soil's parameters in pile design, so that their use predict the real pile response, through inverse analysis of single-pile, statically incremental, *lateral* load test, considering the nonlinearity of both soil and pile. Towards this achievement, algorithm was designed, based on the phenomenological Winkler-type constitutive model BWGG, reformulated with Implicit Finite Difference equations, and embodied with a, derivative-free and MATLAB codified, local minimizer algorithm.

Thesis *layout* follows, summarizing the content of the chapters and appendices:

**Algorithm Design** Algorithm design process and content, along with the assumptions, delimitatins and limitations made, of which the awarenessis is crutial.

**Algorithm Evaluation** The two phases of evaluation. First, its technical adequacy's verification and, afterwards, its physical accuracy's validation.

**Conclusions** Summary of work and proposals of furure relatives themes.

**Matlab Code** The codified algorithm in MATLAB language, along with a brief guide.

**Finite Elements 3D analysis** The analysis used in validation process. Results' report and figures.

# Chapter 2

## Algorithm Design

The algorithm design consists of two parts: designing the forward analysis algorithm and designing the analysis inverse algorithm.

The first is the algorithm of solving the classical laterally loaded pile problem: given the lateral load, and estimating the soil reactions, pile's response is computed. The second allows the inverse process: given pile's response, and the lateral load, parameters that govern the soil reactions are computed, based on the forward analysis and optimization technics.

The codes utilize the phenomenological constitutive model BWGG [1–4] , since it allows the nonlinearity of the soil and the inelasticity of the pile to be expressed in a synoptic, clear way (see p. 7). This constitutive model was implemented through implicit finite-difference equations, as described in the first section of the chapter. Crutial is the awareness of the assumptions, delimitatins and limitations made (section 2.3).

### 2.1 Forward Analysis Algorithm

A laterally loaded single pile is a soil-structure interaction problem, since the soil reaction is dependent on the pile movement, and the pile movement is dependent on the soil reaction. The solution, i.e. the computation of pile's response, must satisfy a nonlinear differential equation as well as equilibrium and compatibility conditions.

In the next paragraphs, a brief background theory on the governal differential equation is presented. Then,  $n$  pile's nodes and  $i$  iterations are introduced, dicretizing the pile and the loading in smaller elements and steps, respectively. Afterwards, implicit finite-difference equations [5] describe the governal differential equation and the boundary

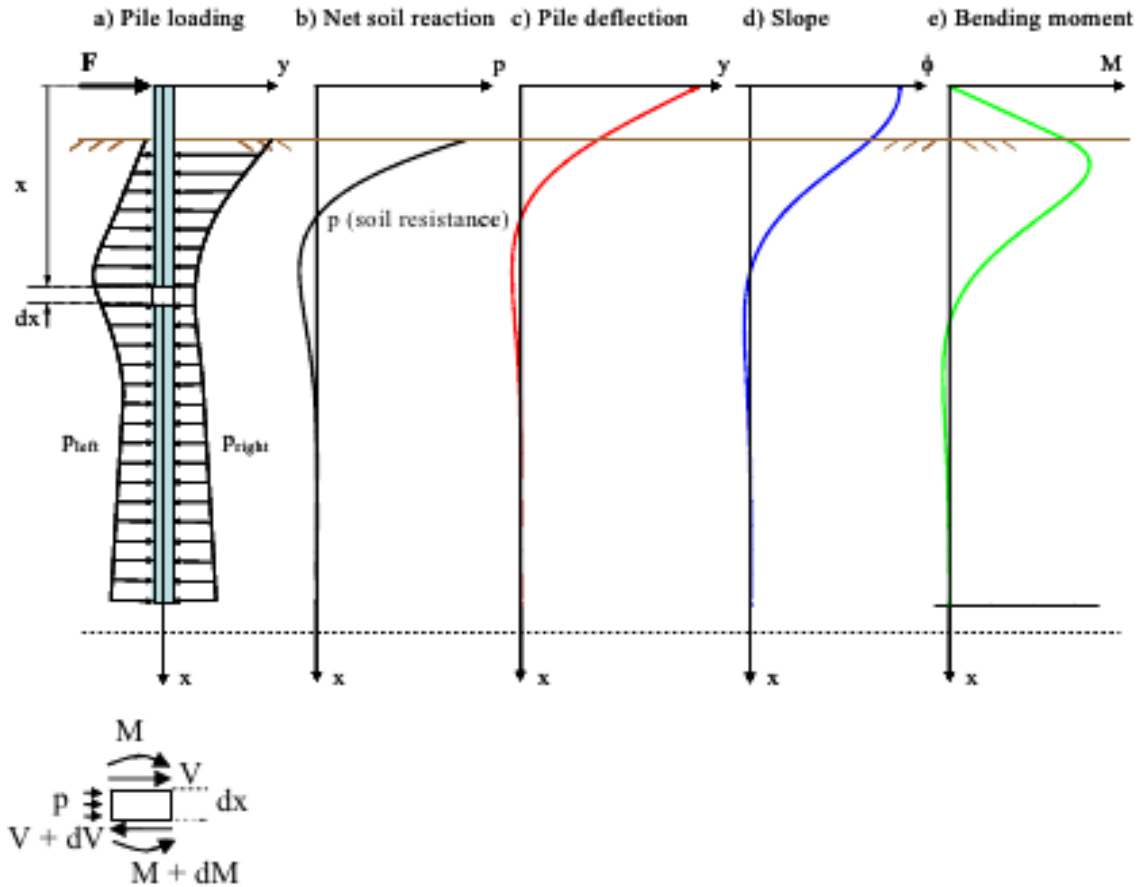


FIGURE 2.1.1: Laterally loaded pile problem

conditions. Nonlinearity of pile and soil is, then, added, using the BWGG model. Finally, all the equations are summarized in a system. The overall process of the algorithm, though, is better understood in the flowchart fig.2.1.5.

**The governal equation** The differential equation is created from the pile's consideration as an elastic, initially, beam and the soil reaction as the distributed load along the beam, derived by Hetenyi (1946) [6]).

This equation can be obtained by considering moment equilibrium of the infinitesimal element of pile length ( $dz$ ) (as shown in figure .2.1.1), and by calculating the bending moment  $M$ , as integral of the normal stresses,  $\sigma_z$ , acting within the cross section of area  $A$  ( $M = \int_A \sigma_z y dA$ ). Its final expression is the eq.2.1.1.

$$\frac{\partial^2}{\partial z^2} \left( EI \frac{\partial^2 y}{\partial z^2} \right) + p = 0 \quad (2.1.1)$$

$$\left\{ \begin{array}{l} M = EI \frac{\partial^2 y}{\partial z^2} \\ Q = \frac{\partial M}{\partial z} \\ q = -\frac{\partial Q}{\partial z} = \frac{\partial^2 M}{\partial z^2} \\ p = -q \end{array} \right.$$

**Dicretization of pile and loading:**  $n$  nodes,  $i$  iterations

$$p_{n,i} = k_{n,i} y_{n,i} \quad (2.1.2)$$

$$\begin{aligned} 0 &= \frac{\partial^2}{\partial z^2} \left( EI \frac{\partial^2 y}{\partial z^2} \right) + ky \\ &= \frac{\partial^2 EI}{\partial z^2} \frac{\partial^2 y}{\partial z^2} + EI \left( \frac{\partial^4 y}{\partial z^4} \right) + ky \\ &\approx \left( \frac{EI_{n-1,i} - 2EI_{n,i} + EI_{n+1,i}}{\Delta z^2} \right) \left( \frac{y_{n-1,i} - 2y_{n,i} + y_{n+1,i}}{\Delta z^2} \right) \\ &\quad + EI_{n,i} \left( \frac{y_{n-2,i} - 4y_{n-1,i} + 6y_{n,i} - 4y_{n+1,i} + y_{n+2,i}}{\Delta z^4} \right) + k_{n,i} y_{n,i} \\ \Leftrightarrow 0 &= y_{n-2,i} + y_{n-1,i}(-4 + t_1) + y_{n,i}(6 + \frac{k_{n,i} \Delta z^4}{EI_{n,i}} - 2t_1) \\ &\quad + y_{n+1,i}(-4 + t_1) + y_{n+2,i} \end{aligned} \quad (2.1.3)$$

$$\text{whereas } t_1 = \frac{EI_{n-1,i} - 2EI_{n,i} + EI_{n+1,i}}{EI_{n,i}}$$

## Boundary conditions

**Head of Pile**  $z \equiv z_{Head} = 0 \Leftrightarrow node = 3^1$

- $Q = P_{lateral\ load}$

$$\begin{aligned}
 P &= \frac{\partial M}{\partial z} \\
 &= \left[ \frac{\partial}{\partial z} \left( EI \frac{\partial^2 y}{\partial z^2} \right) \right]_{z=0} \\
 &= \left[ \frac{\partial EI}{\partial z} \frac{\partial^2 y}{\partial z^2} + EI \left( \frac{\partial^3 y}{\partial z^3} \right) \right]_{z=0} \\
 &\approx \left( \frac{EI_{4,i} - EI_{2,i}}{2\Delta z} \right) \left( \frac{y_{2,i} - 2y_{3,i} + y_{4,i}}{\Delta z^2} \right) \\
 &\quad + EI_{3,i} \left( \frac{-y_{1,i} + y_{2,i} - y_{4,i} + y_{5,i}}{2\Delta z^3} \right) \\
 \Leftrightarrow \frac{P2\Delta z^3}{EI_{3,i}} &= -y_{1,i} + y_{2,i}(2 + t_2) + y_{3,i}(-2t_2) \\
 &\quad + y_{4,i}(-2 + t_2) + y_{5,i} \\
 \text{whereas } t_2 &= \frac{EI_{4,i} - EI_{2,i}}{EI_{3,i}}
 \end{aligned} \tag{2.1.4}$$

- $M = 0$

$$\begin{aligned}
 0 &= \left[ \left( EI \frac{\partial^2 y}{\partial z^2} \right) \right]_{z=3} \\
 \Leftrightarrow 0 &= y_{2,i} - 2y_{3,i} + y_{4,i}
 \end{aligned} \tag{2.1.5}$$

**Pinpoint of Pile**  $z \equiv z_{Head} = L \Leftrightarrow node = NumLayers = nn - 2$

- $Q = 0$

$$\begin{aligned}
 0 &= \left[ \left( EI \frac{\partial^3 y}{\partial z^3} \right) \right]_{z=L} \\
 \Leftrightarrow 0 &= -y_{nn-4,i} + 2y_{nn-3,i} - 2y_{nn-1,i} + y_{nn,i}
 \end{aligned} \tag{2.1.6}$$

- $M = 0$

$$\begin{aligned}
 0 &= \left[ \left( EI \frac{\partial^2 y}{\partial z^2} \right) \right]_{z=L} \\
 \Leftrightarrow 0 &= y_{nn-3,i} - 2y_{nn-2,i} + y_{nn-1,i}
 \end{aligned} \tag{2.1.7}$$

---

<sup>1</sup>Physical nodes' number = pile's layers' number ( $NumLayers$ ). Whilst, total number of nodes  $nn \neq NumLayers$ , but  $nn = NumLayers + 4$ , since 4 plasmatic nodes are created (see last assumption on p.13)

**Non-Linearity** Using the BWGG model, whose parameters  $n, a, b, g$  control the p-y curve (figures 2.1.3, 2.1.2, 2.1.4, [3]). The  $\zeta$  parameters define the nonlinear response, i.e pile's bending moment  $M = \alpha_p EI \frac{\partial^2 y}{\partial z^2} + (1 - \alpha_p) M_y \zeta_p$  and soil reaction (per length)  $p = \alpha_s k_x y + (1 - \alpha_s) p_y \zeta_s$ .

**Pile**  $\kappa$ :curvature

$$\begin{aligned}\kappa &= \frac{\partial^2 y}{\partial z^2} \\ &\approx \frac{y_{n+1,i} - 2y_{n,i} + y_{n-1,i}}{\Delta z^2} \\ d\kappa &= \kappa_{n,i+1} - \kappa_{n,i}\end{aligned}$$

$$\begin{aligned}\frac{d\zeta_p}{d\kappa} &= \frac{1 - |\zeta_p|^{n_p} (b_p + g_p \text{sign}(d\kappa) d\zeta_p)}{\kappa_o} \\ \zeta_{p(n,i+1)} &= \zeta_{p(n,i)} + d\zeta_p \\ EI_{n,i} &= \alpha_p EI_{o(n,i)} + (1 - \alpha_p) EI_{o(n,i)} \{1 - |\zeta_p|^{n_p} (b_p + g_p \text{sign}(d\kappa) d\zeta_p)\} \quad (2.1.8)\end{aligned}$$

**Soil**

$$dy = y_{n,i+1} - y_{n,i}$$

$$\begin{aligned}\frac{d\zeta_s}{dy} &= \frac{1 - |\zeta_s|^{n_s} (b_s + g_s \text{sign}(dy) d\zeta_s)}{y_o} \\ \zeta_{s(n,i+1)} &= \zeta_{s(n,i)} + d\zeta_s \\ k_{n,i} &= \alpha_s k_{o(n,i)} + (1 - \alpha_s) k_{o(n,i)} \{1 - |\zeta_s|^{n_s} (b_s + g_s \text{sign}(dy) d\zeta_s)\} \quad (2.1.9)\end{aligned}$$

**Lateral pile displacements in all depths** The system of equations is completed, in the following page, whereas:

$$\begin{aligned}kk_{n,i} &= 6 + \frac{k_{n,i} 2\Delta z^4}{EI_{n,i}} \\ t_1 &= \frac{EI_{n-1,i} - 2EI_{n,i} + EI_{n+1,i}}{EI_{n,i}} \\ t_2 &= \frac{EI_{4,i} - EI_{2,i}}{EI_{3,i}}\end{aligned}$$

$$\begin{array}{cccccccccccccccccc}
 & 1 & 2 & 3 & 4 & 5 & \dots & n-2 & n-1 & n & n+1 & n+2 & \dots & nn-4 & nn-3 & nn-2 & nn-1 & nn \\
 \text{2.1.4} & \left( \begin{array}{ccccccccccccccccc}
 -1 & 2+t_2 & -2t_2 & -2+t_2 & 1 & \dots & 0 & 0 & 0 & 0 & 0 & \dots & 0 & 0 & 0 & 0 & 0 & 0 \\
 0 & 1 & -2 & 1 & 0 & \dots & 0 & 0 & 0 & 0 & 0 & \dots & 0 & 0 & 0 & 0 & 0 & 0 \\
 \vdots & \vdots & \vdots & \vdots & \vdots & \dots & \vdots & \vdots & \vdots & \vdots & \vdots & \dots & \vdots & \vdots & \vdots & \vdots & \vdots & \vdots \\
 \text{2.1.3} & \left( \begin{array}{ccccccccccccccccc}
 0 & 0 & 0 & 0 & 0 & \dots & 1 & -4+t_1 & kk_{n,i} & -4+t_1 & 1 & \dots & 0 & 0 & 0 & 0 & 0 & 0 \\
 \vdots & \vdots & \vdots & \vdots & \vdots & \dots & \vdots & \vdots & \vdots & \vdots & \vdots & \dots & \vdots & \vdots & \vdots & \vdots & \vdots & \vdots \\
 \text{2.1.7} & \left( \begin{array}{ccccccccccccccccc}
 0 & 0 & 0 & 0 & 0 & \dots & 0 & 0 & 0 & 0 & 0 & \dots & 0 & 1 & -2 & 1 & 0 & 0 \\
 0 & 0 & 0 & 0 & 0 & \dots & 0 & 0 & 0 & 0 & 0 & \dots & -1 & 2 & 0 & -2 & 1 & 0
 \end{array} \right) \right)
 \end{array}$$

$$* \left\{ \begin{array}{c} y_1 \\ y_2 \\ \vdots \\ y_n \\ \vdots \\ y_{nn-1} \\ y_{nn} \end{array} \right\} = \left\{ \begin{array}{c} \frac{P 2 \Delta z^3}{EI_{3,i}} \\ 0 \\ \vdots \\ 0 \\ \vdots \\ 0 \\ 0 \end{array} \right\}$$

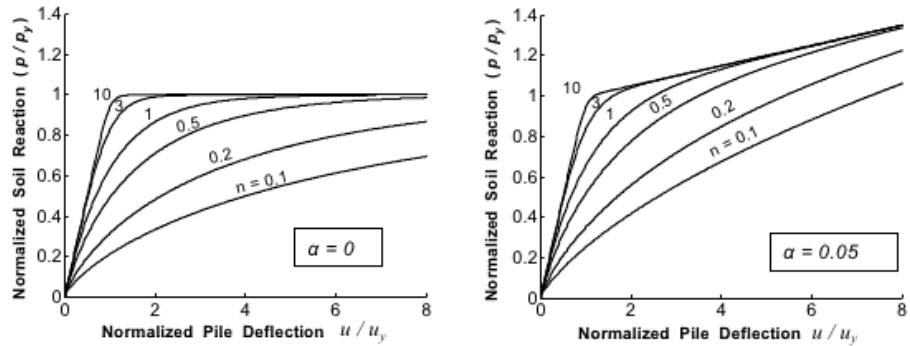


FIGURE 2.1.2: Effect of “n” parameter on the sharpness of the transition from the linear to nonlinear range during virgin loading

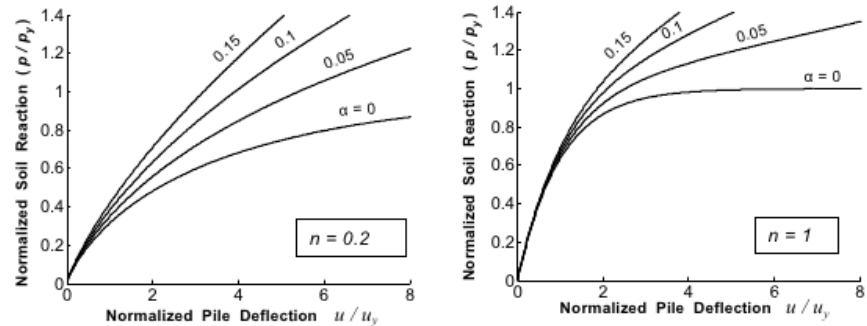


FIGURE 2.1.3: Effect of the “a” parameter, control of the post yielding shear stiffness

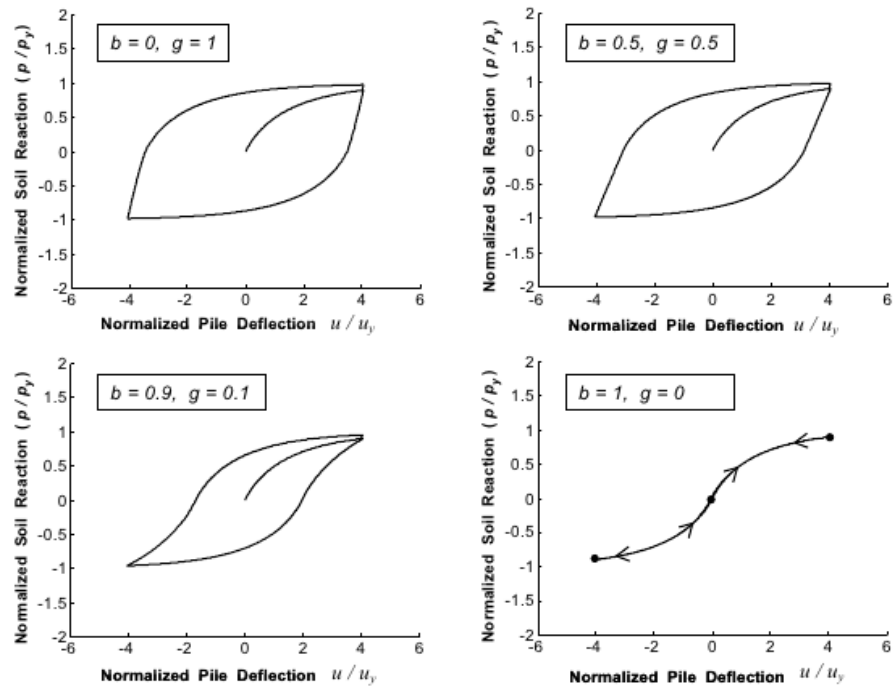


FIGURE 2.1.4: Effect of “b”, “g” parameters on the unloading-reloading curve shape

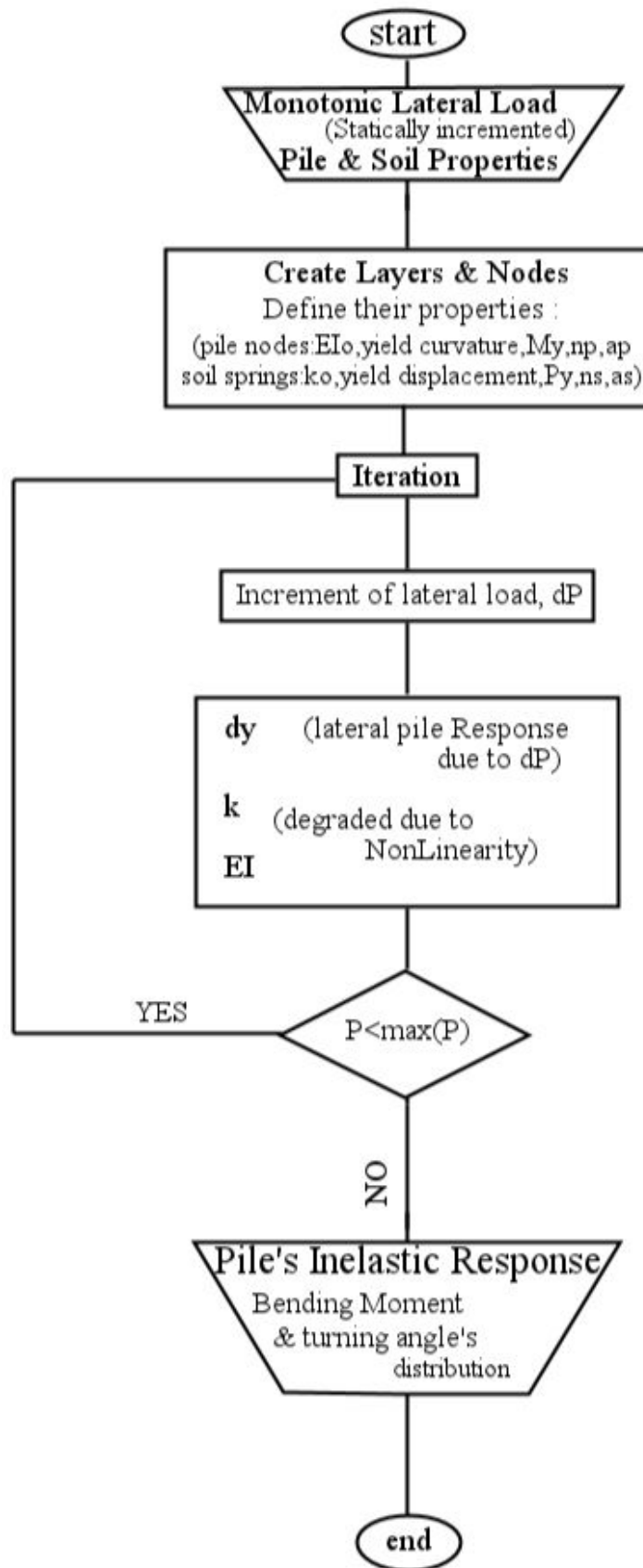


FIGURE 2.1.5: Forward analysis flowchart

## 2.2 Inverse Analysis Algorithm

In inverse analysis, constitutive parameter values are optimized in the way that the error/deviation between the recorded response, by insitu measurements, and the computed data is minimized. The process is better understood in the flowchart fig.2.2.2.

Output are the optimized parameters:  $k_o$ , the initial, refference, soil spring stiffness,  $m$ , the power that determines the way soil stiffness differs in depth and is critical [7] to the pile's response,  $n$ , the BWGG parameter (p. 9) and  $Py$ , the ultimate soil reaction.

**Optimization techniques** *Unconstrained nonlinear* optimization was used, i.e. finding the minimum of a scalar function (the error) of several variables, starting at an initial estimate, without the user to define upper and lower limits of the variables.

The MATLAB<sup>®</sup> function “fminsearch” was selected, which is a local minimize and uses the, derivative-free, Nelder-Mead simplex algorithm. This function uses the simplex search method of Lagarias et al. (1998, [8]). This is a direct search method that does not use numerical or analytic gradients.

The way it operates, in summary, is: If  $n$  is the length of vector  $x$  ( $n$  are the parameteres to be optimized), a simplex in  $n$ -dimensional space is characterized by the  $n + 1$  distinct vectors that are its vertices.“ In two-space, a simplex is a triangle; in three-space, it is a pyramid. At each step of the search, a new point in or near the current simplex is generated. The function value at the new point is compared with the function’s values at the vertices of the simplex and, usually, one of the vertices is replaced by the new point, giving a new simplex. This step is repeated until the diameter of the simplex is less than the specified tolerance”, fig.2.2.1 [9].

Scaling the variables and the subject function was also nesseccary for numerical “equality” [10].

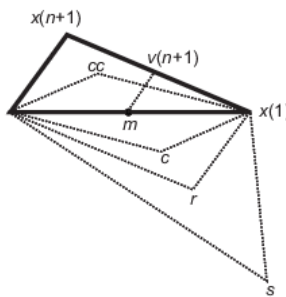


FIGURE 2.2.1: A graphical simplified explanation of the calculations that fminsearch does in the procedure, along with each possible new simplex. The original simplex has a bold outline. The iterations proceed until they meet the stopping criterion.

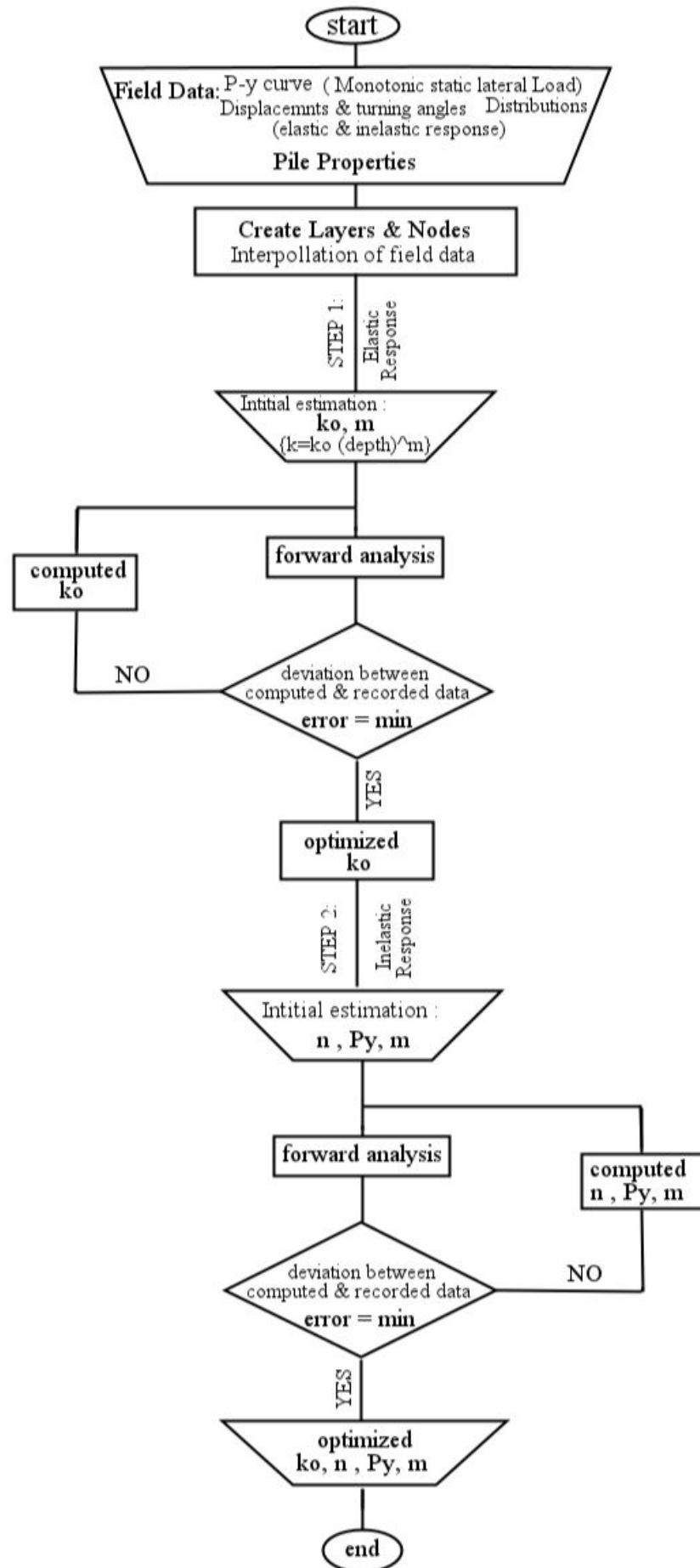


FIGURE 2.2.2: Inverse analysis flowchart

## 2.3 Assumptions, Delimitations and Limitations

### Assumptions

- Lateral, static and monotonic load of single pile.
- Soil drained, single-layered, homogenous but not uniform, modelised by Winkler-type nonlinear springs ( $p = ky$ , fig. 2.3.1, [6]). The soil spring stiffness ( $k$ ) is increased in depth ( $z$ ) in an optimum way ( $k(z) = k^{ref} * z^m$ , whereas  $m$  is part of the output) and is decreased during the loading stages due to nonlinearity (eq. 2.1.9).
- Pile's nonlinearity of the flexural stiffness (eq. 2.1.8).
- Free pile head.
- Four plasmatic nodes are created in analysis because of the finite difference method's approach of the 4th grade governal equation (eq.2.1.1), two above the head of pile and two below its pinpoint, with properties of the nearest physical node.

### Delimitations

- Cycling loading is not supported. Thus, load-induced anisotropy, seperation (gapping) of the pile from the soil (figure 2.3.2, [11]) and cyclic strength degration (figure 2.3.3, [1]) are not expressed.
- Dynamic loading is also not supported. Thus, damping (hysteretic and radiation) is not expressed. The reason of excluding cyclic and dynamic analysis is the reduction of the parameters that will be optimized. However, the static analysis excludes the time-domain analysis and, therefore, the explicit expression of finite difference method, leading to the, more complicate, implicit expression in the design.
- The effect of the pile cross-section shape (Reese and Van Impe, 2001, figure 2.3.4, [6]) and the surface roughness are not considered.
- Vertical load was from self-weight and was considered negligible.

### Limitations

- Quality of the output depends on the quality of the input: the recorded pile response and the initial estimation of the wanted parameters. The first is affected

by the type and methodology of measurement instrumentation and the pile's installation conditions, for field-harvested data, or by the simulation's assumptions, for simulation-harvested data. Due to the local minimizer used in the optimization, for numerical balance and speed, necessary is a rational initial estimation, i.e. positive parameters within the range of bibliographical records.

- Because of the spatial sensitivity of the finite difference method, the pile's plastic hinge leads to numerical imbalance, since the part of pile above the hinge deflects, then, independently and unconnected to the part below the hinge. Thus, the lateral load could be big enough to provoke inelastic pile response, but not reach ultimate level.
- Due to the macroscopic approach, stresses, strains and the related microscopic quantities are not computed.
- The continuous nature of the soil is not explicitly modeled, since soil is simulated by a series of nonlinear springs.

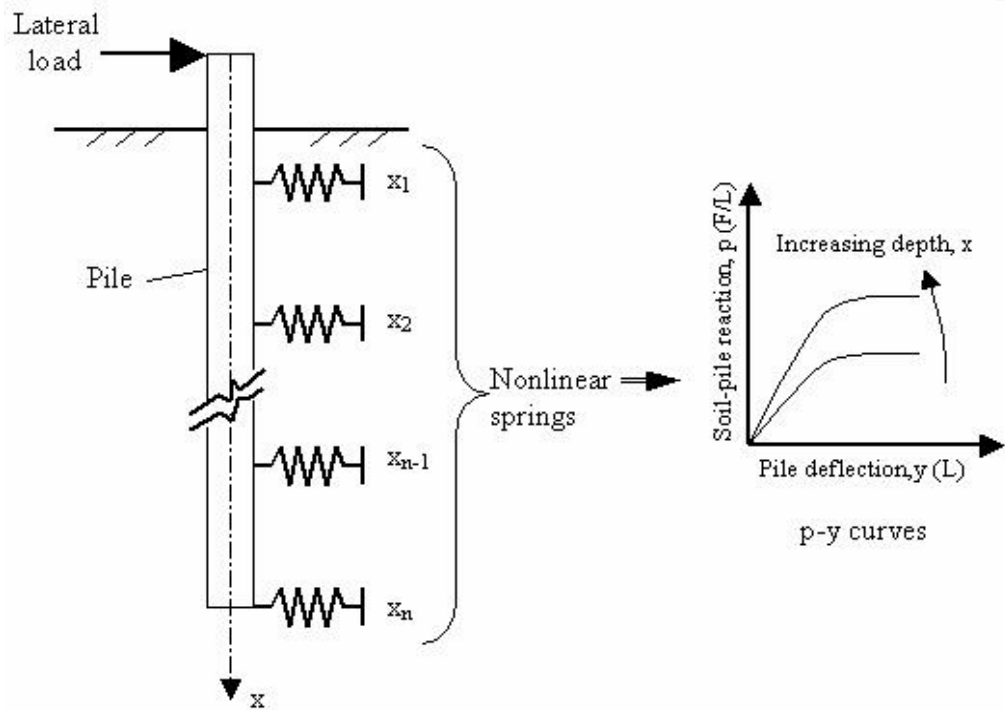


FIGURE 2.3.1: Winkler-type nonlinear soil model

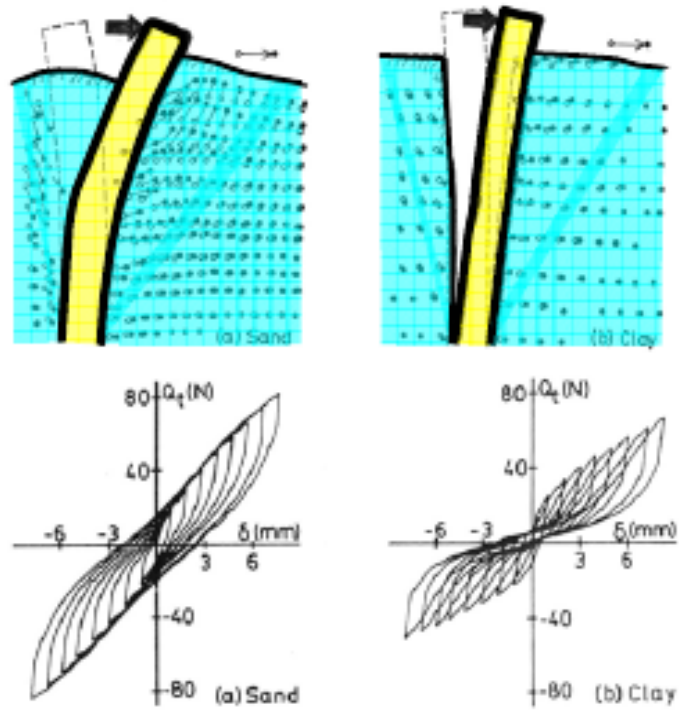


FIGURE 2.3.2: Pile's response to cyclic lateral load in cohesion-less (left) and cohesive (right) soil.

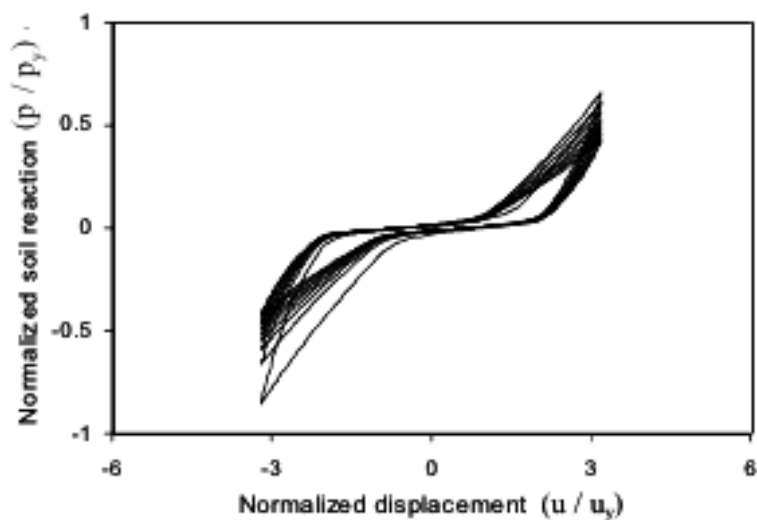


FIGURE 2.3.3: Hysteretic component of a typical soil reaction on a pile in stiff clay with gapping effect and strength deterioration, computed with the BWGG model

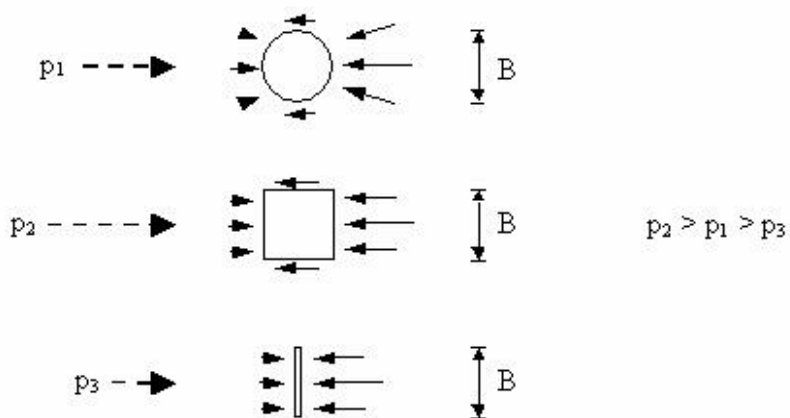


FIGURE 2.3.4: The influence of pile's cross-sectional shape on the soil reaction  $p$

# Chapter 3

## Algorithm Evaluation

The designed algorithm was evaluated in two phases. First, its technical adequacy was verified and, afterwards, the physical accuracy was validated.

### 3.1 Verification

Through the verification process, technical adequacy, in terms of performance, stability and velocity, was examined. Time-consuming functions and code's "hot-spots", regions where high proportion of executed instructions occur, were minimized. Simplicity and articulacy in the input demand and the output expression were, also, examined. In the required multiple analyses, pile responses, created with the forward analysis algorithm, were used as data source. Thus, the ability of adjustment in the unknown soil behaviour has not evaluated yet,in this phase.

Such an inverse analysis is presented in the following subsections.

#### 3.1.1 Input data creation

Major input of the inverse analysis is the pile's response to lateral load and soil reaction.

This response, expressed by the curves of load-head displacement ( $p - y$ ) and depth-displacement ( $z - y$ ), was created by the forward analysis algorithm implementation, using as input the values of table 3.1.1.

TABLE 3.1.1: Forward Analysis Input

	geometry	$L = 24 \text{ m}$ $d = 1 \text{ m}$
pile		$E = 21 \text{ GPa}$
	strength	$M_y = 4000 \text{ kNm}$ $\alpha_p = 0.001$
		$k_o^{ref} = 30 \text{ MN/m}^2$
soil	$k_o = k_o^{ref} * depth^m$	$m = 1$ $P_y = 400 \text{ kN}$ $n = 0.6$ $\alpha_s = 0.001$
load	maximum iterations	$P = 1500 \text{ kN}$ 1000

TABLE 3.1.2: Verification Case Input

	geometry	$L = 24 \text{ m}$ $d = 1 \text{ m}$
pile		$E = 21 \text{ GPa}$
	strength	$M_y = 4000 \text{ kNm}$ $\alpha_p = 0.001$
		$k_o^{ref} = 100 \text{ MN/m}^2$
soil	(initial estimation)	$m = 0.5$ $P_y = 500 \text{ kN}$ $n = 0.5$
		$\alpha_s = 0.001$
	analysis's iterations	1000
	pile's response	$p - y$ curve $z - y$ curve

TABLE 3.1.3: Verification Case Output

```

OPTIMIZATION results:
The no.1 Soil Material has n=0.6 .
The no.1 Soil Material has Pyo=395.583 kN.
The no.1 Soil Material has ko=30000 kN/m2.
The no.1 Soil Material has power (kx=ko*depth^power)=1.
Elapsed time is 145.744490 seconds.

```

### 3.1.2 Inverse analysis

When inverse analysis code was executed, using as input the values of table 3.1.2, the output graphical figures 3.1.2 and 3.1.3 were created, in which blue represent the calculated and red the recorded, given in input, data.

Synopsis of the optimized soil parameteres, was displayed, then, on the Command Window of the MATLAB® environment, as showed in table 3.1.3.

### 3.1.3 Output assessment

Assessing the results, absolute curve fitting and 98% ~ 100% accuracy in defining the wanted soil parameteres were achieved, as expected by a refeed analysis. Results were expressed in both, user-friendly, text and graphical way. Analysis lasted less than three minutes.

Reffering to time, counter is activated, when **OK** bottom of the pile's input dialog box (figure 3.1.1 ) is pressed, and gets deactivated, when optimization and graphs creation are completed. Moreover, the code was runned through the CloudFront service of the NTUA's Computer Center and, thus, its hardware was used, boosting velocity.

On the other hand, despite of the above good technical results, refeed analyses can not test the physical accuracy. Thus, additional analysis, using , even simulation's, experimental results was imperative and is presented in the following section.

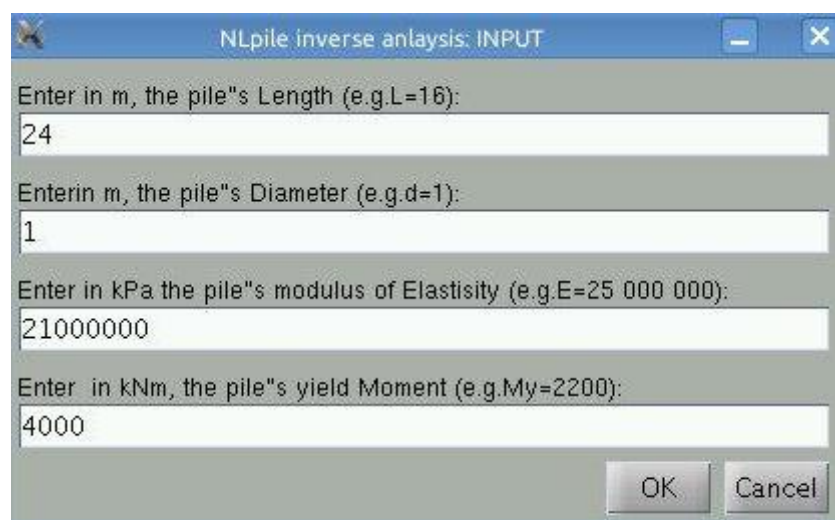
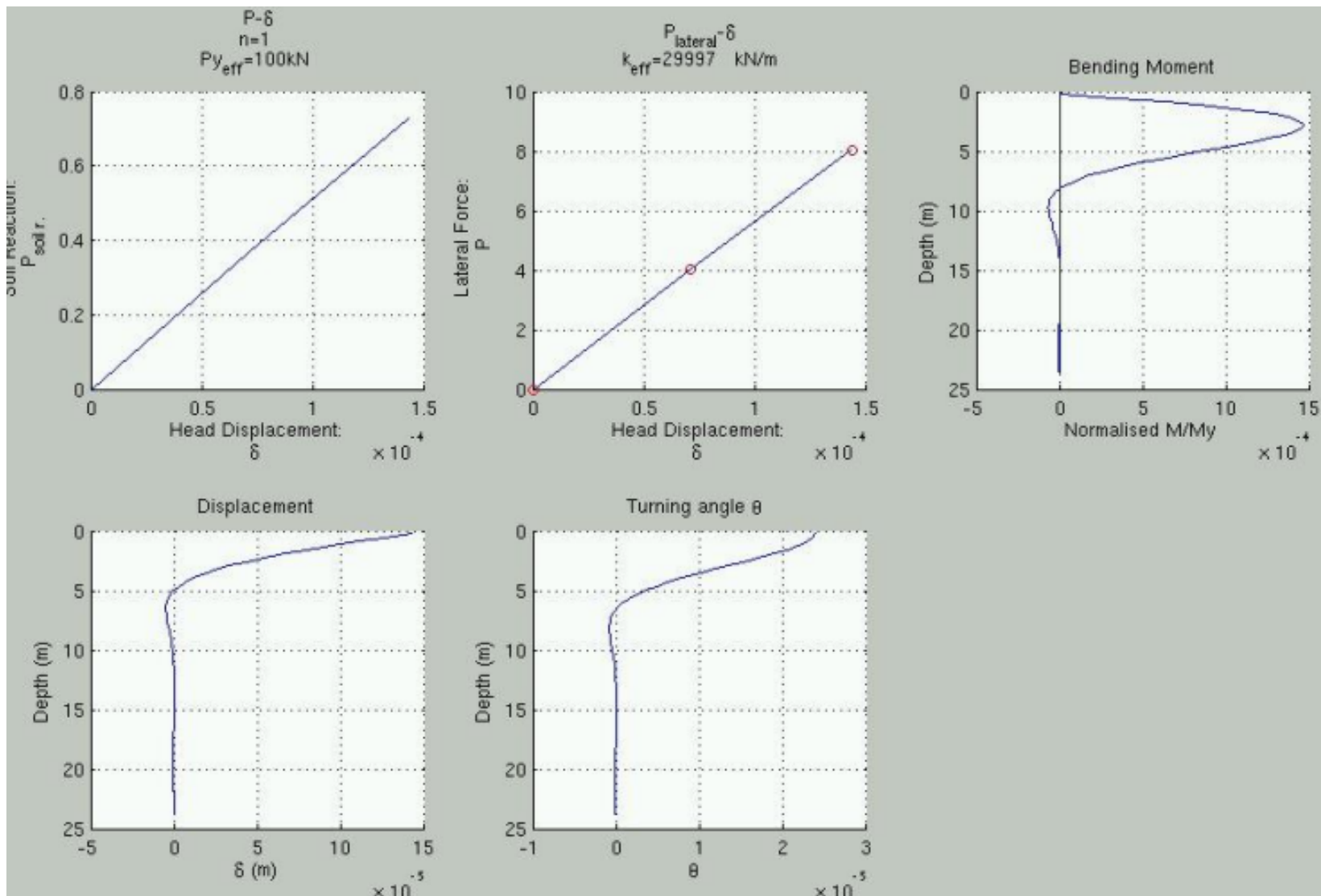


FIGURE 3.1.1: Verification case: Dialog box gathering input

FIGURE 3.1.2: Verification case: optimum  $k_{elastic}$

### 3.1 Verification

21

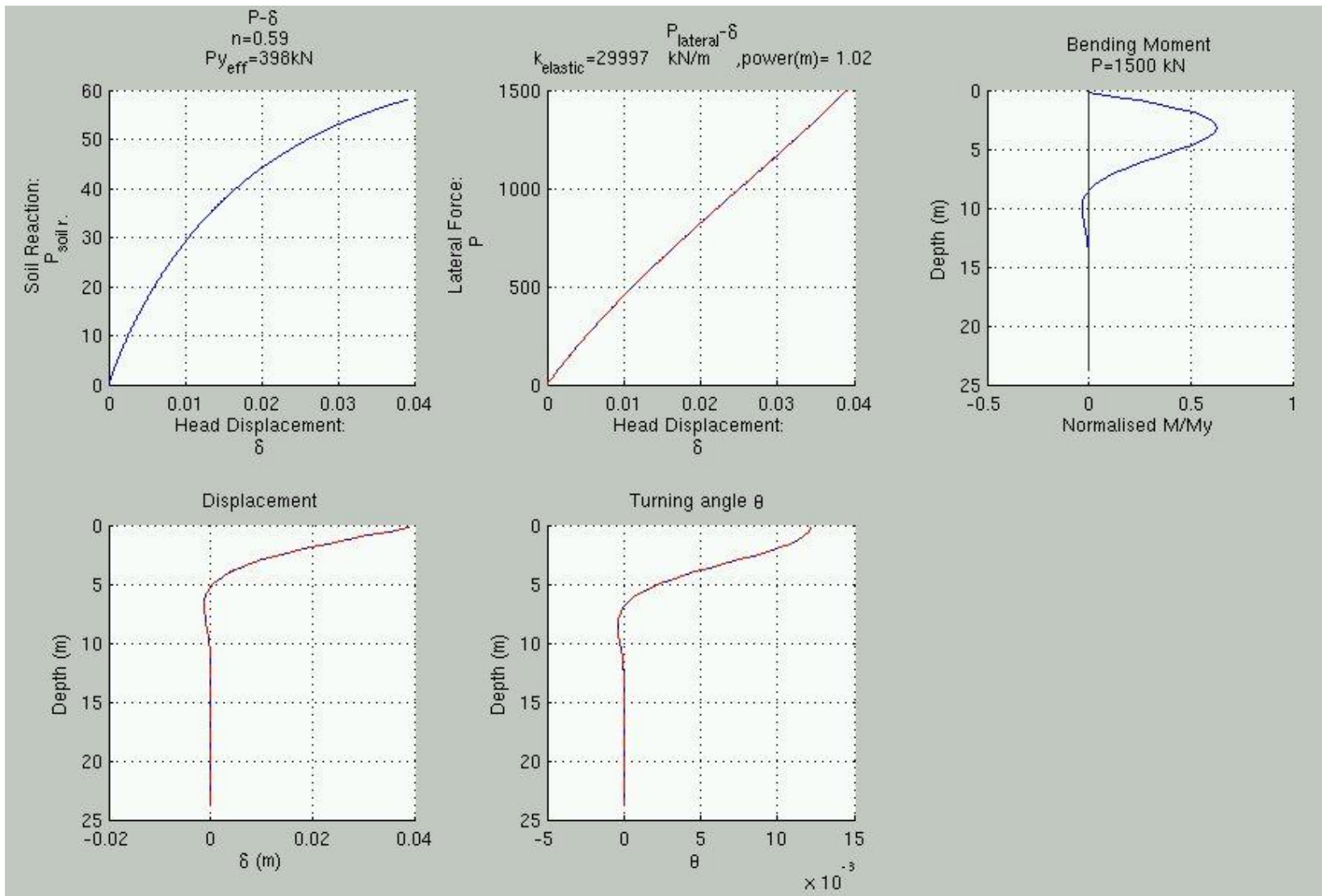


FIGURE 3.1.3: Verification case: optima  $n, P_y, m$

## 3.2 Validation

Through the validation process, physical accuracy, in macroscopic terms, was examined. This accuracy was measured by the fitting rate of the calculated response into the recorded pile behaviour and by the relationship of the optimized soil parameters to the parameters proposed in empirical methods.

In situ static lateral load test was numerically simulated in Finite Elements Method (FEM) software, PLAXIS 3D<sup>©</sup>. The simulation, its result's implementation into the inverse algorithm and the output assessemnt are presented in the following subsections.

### 3.2.1 Input data creation

“Recorded” pile behaviour was created by numerical simulation of the, lateral load, pile test.

Four materials were defined, fig.3.2.2, detailly reported in Appendix ???. The *Soil* material was following the Hardening Soil constitutive model [12]. The reinforced concrete *Pile* was simulated by soil-interface Mohr-Coulomb elements. The *Head* of the pile was simulated by plate material and the *Inclinometer* in pile axis by beam elements, which modulus of elasticity is the  $\frac{1}{10000}$  of the pile's modulus, so as not to affect the pile's deflection.

In particular for the reinforced concrete pile, concrete was assumed to have characteristic strength ( $f_{ck}$ )  $30 \text{ MPa}$ , the steel strength  $500 \text{ MPa}$  (*S500s* or *StIV*) and the steel bar section area percentage ( $\rho$ ) to be  $1.5\%$ . Proposed values, which determine failure envelope in the M-N space, are the cohesion ( $c$ )  $15262 \text{ kPa}$  and the tensible strength ( $\sigma_t$ )  $7534 \text{ kPa}$  [13]. From this envelope, fig.3.2.4, without axial force ( $N = 0 \text{ MN}$ ), the yield moment ( $M_y$ ) of the pile is  $2200 \text{ kNm}$ .

**Brom's method confirmation** An interesting notice over the figure 3.2.1, which showes the soil's plastic points created during the loading stages, is that the prolongation of line that delimits the plastified soil, in the side of the passive pressure, leads to the plastic hinge of pile. This is a confirmation of Broms' method (1964) over the single, long, free-head pile in cohesionless soil. According to which, the ultimate soil resistance develops from the ground surface to the point of plastic hinge, till the depth  $f$  [14]. Moreover, at this point the shear is zero and the bending moment is maximum . Thus, depth  $f$  is computed by solving the system of the moments balance and the horizontal forces balance at the hinge depth, i.e.  $Hf = M_y + \frac{f}{3} \frac{3d\sigma'_v k_p f}{2}$ ,  $H = \frac{3d\sigma'_v k_p f}{2}$  (fig. 3.2.3b, [15]). In this case,  $f = 3,2 \text{ m}$  (Broms' method), close to the  $f = 3,6 \text{ m}$  (3D FEM).

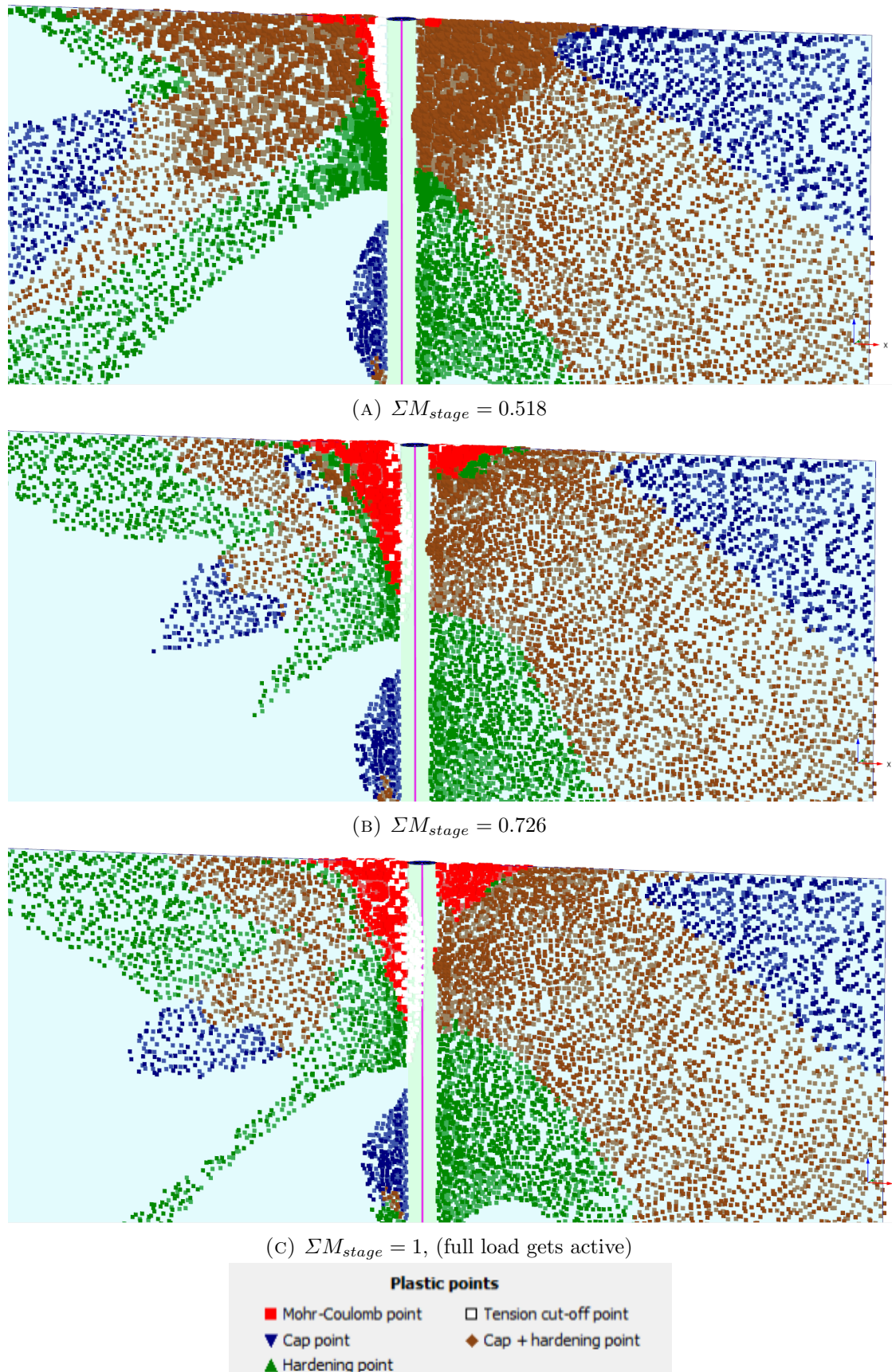


FIGURE 3.2.1: 3D Finite Element Analysis: Plastic points

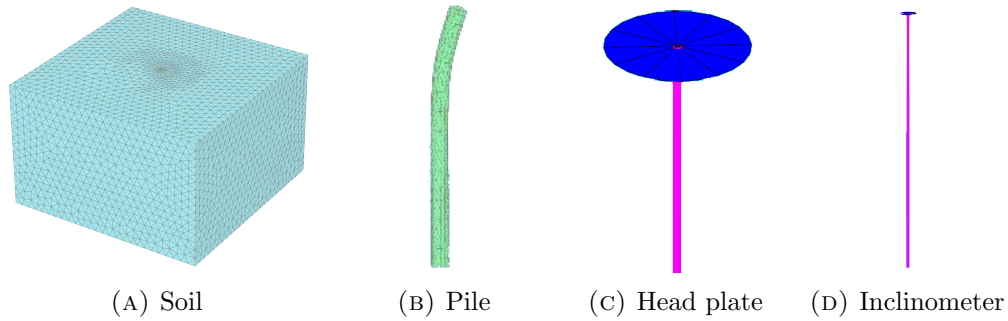


FIGURE 3.2.2: 3D Finite Element Analysis: Material elements

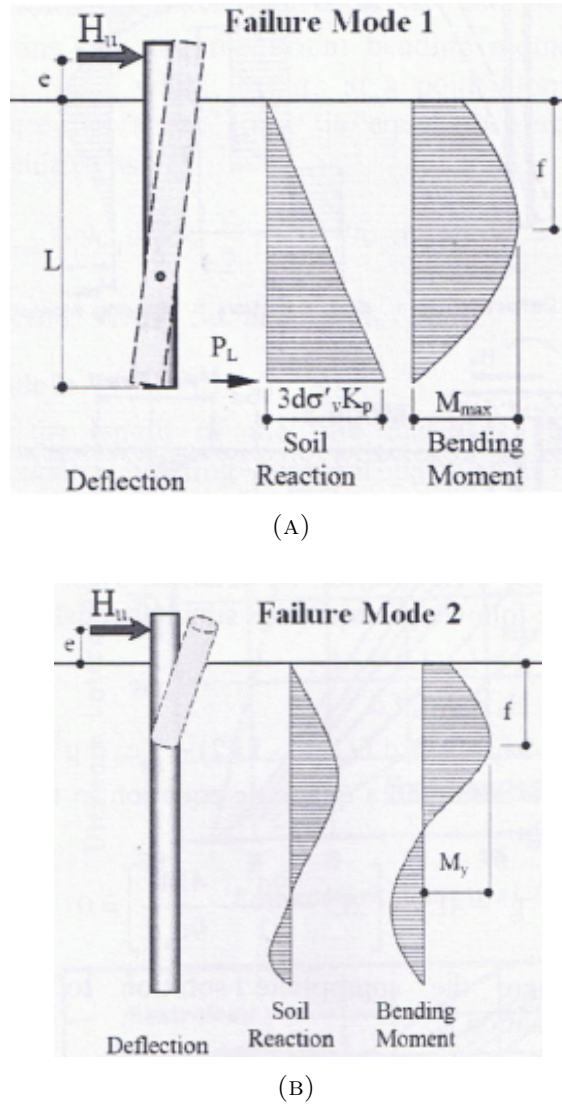
FIGURE 3.2.3: Brom's method for analysis of single, unrestrained against rotation, piles in cohesionless soil, whereas  $\sigma'_v = \gamma'z$  is the active vertical stress and  $K_p = \tan^2(45 + \frac{\phi}{2})$  is the coefficient of passive earth pressure, (Rankine 1857)

TABLE 3.2.1: 3D Finite Elements Analysis Input

pile	geometry	$L = 16 \text{ m}$
		$d = 1 \text{ m}$
strength		$E = 25 \text{ GPa}$
		$c = 15262 \text{ kPa}$
soil		$\sigma_t = 7534 \text{ kPa}$
		drained
parameters		$\gamma = 20 \text{ kN/m}^3$
		$\phi = 32^\circ$
HS model		$E_{50}^{ref} = 50\,000 \text{ kN/m}^2$
parameters		$m = 0.5$
head	plate	$E = 25 \text{ GPa}$
inclinometer	beam	$E = 2,5 \text{ MPa}$

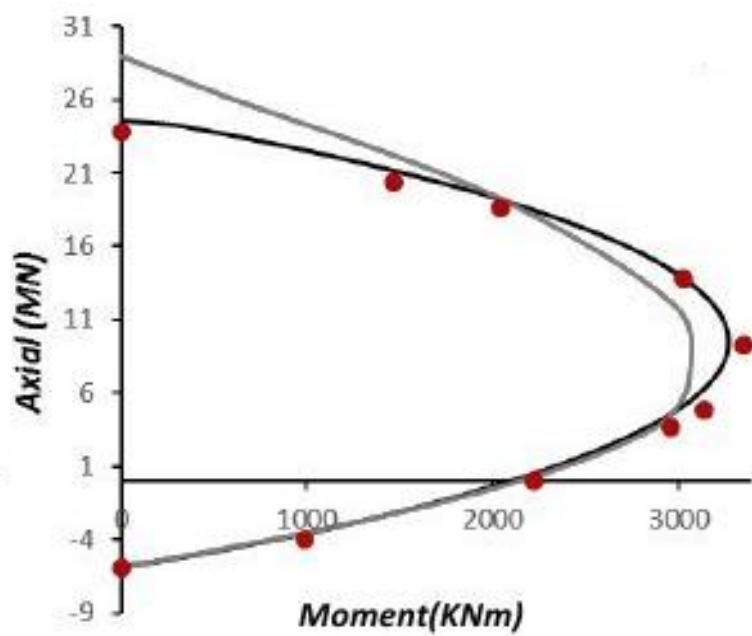


FIGURE 3.2.4: M-N failure envelope of the reinforced concrete pile

### 3.2.2 Inverse analysis

When inverse analysis code was executed, using as input the values of table 3.2.3, the output graphical figures, fig.3.2.6 and fig.3.2.7, were created, in which blue and continues lines (i.e. —) represent the calculated data, whilst the circular red points (i.e. ○) and the broken ( i.e. -- ) lines represent the recorded, given as input, data.

Synopsis of the optimized soil parameteres, was displayed, then, on the Command Window of the MATLAB<sup>®</sup> environment, as showed in table 3.2.2.

### 3.2.3 Output assessment

The physical rightness, in terms of the fitting rate of the calculated response into the recorded pile behaviour, is adequately confirmed in fig.3.2.7.

A numerical assessement could be only indirect, in contrast to the verification case, since the “correct” soil parameters are not distinctly predictable. To begin with, the soil spring’s initial stiffness  $k_o$  is within the, bibliographically proposed, range for cohesionless materials, and specifically for, relatively dense, sand ([16], combined with the Makris & Gazetas, 1992, relationship  $k_s = 1.2 E_s$ ). The exponential power  $m = 0.5$ , which defines the distribution of  $k$  with depth, seems logical for cohesionless material [7]. The  $n = 0.75$  for the parameter, that governs the sharpness of transition from the linear to nonlinear range during initial loading, intuitively only, seems logical. Last but not least, the ultimate, reference ( when depth  $z = 1 m$ ), soil reaction  $P_{yo} = 127 kN$ , is also within the bibliographical range [11], since  $127 = 1.95 \tan^2(45 + \frac{32}{2})20$ , using Broms (1964) expressions.

TABLE 3.2.2: Validation Case Output

<pre> OPTIMIZATION results: The no.1 Soil Material has n=0.75 . The no.1 Soil Material has Pyo=127.188 kN. The no.1 Soil Material has ko=53938 kN/m2. The no.1 Soil Material has power(kx=ko*depth^power)=0.5 . Elapsed time is 467.561652 seconds. </pre>
------------------------------------------------------------------------------------------------------------------------------------------------------------------------------------------------------------------------------------------------------------

TABLE 3.2.3: Validation Case Input

pile	geometry	$L = 16 \text{ m}$
		$d = 1 \text{ m}$
strength		$E = 25 \text{ GPa}$
		$M_y = 2200 \text{ kNm}$
soil (initial estimation)		$\alpha_p = 0.001$
		$k_o^{ref} = 100 \text{ MN/m}^2$
soil (initial estimation)		$m = 0.5$
		$P_y = 500 \text{ kN}$
soil (initial estimation)		$n = 0.5$
		$\alpha_s = 0.001$
pile's response	(Appendix B.1.1 ) (Appendix B.1.2 )	$p - y$ curve $z - y$ curves

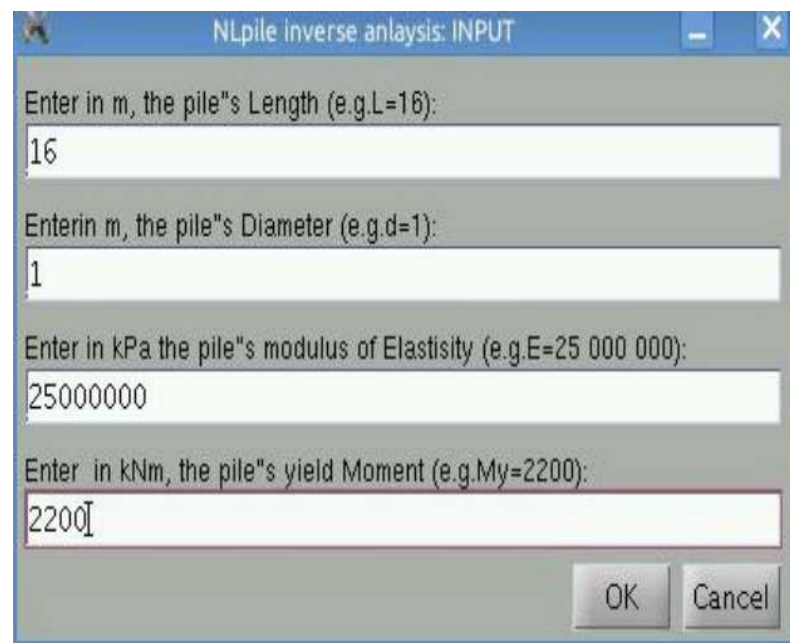
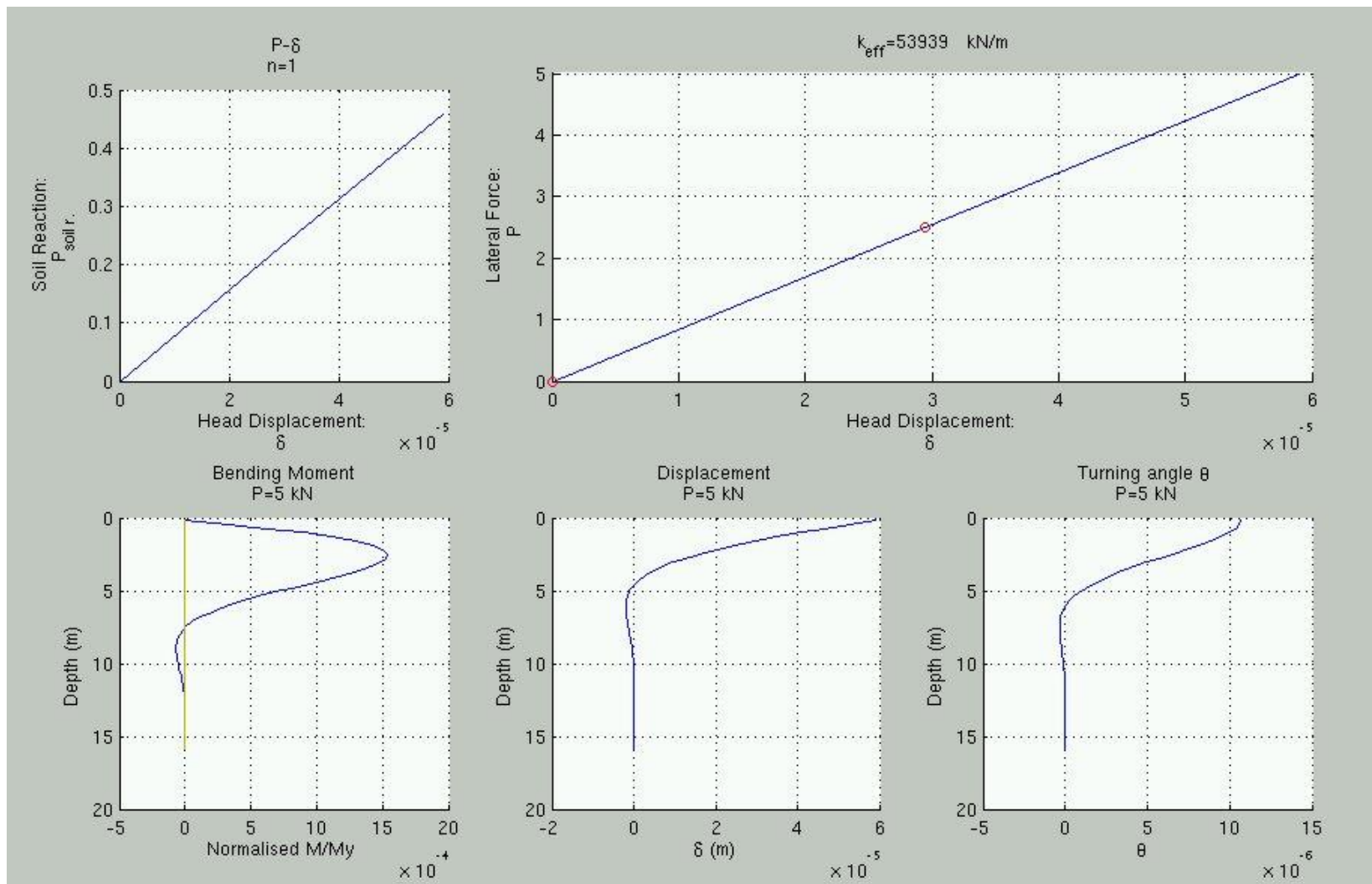


FIGURE 3.2.5: Validation case: Dialog box gathering input

FIGURE 3.2.6: Validation case: optimum  $k_{elastic}$

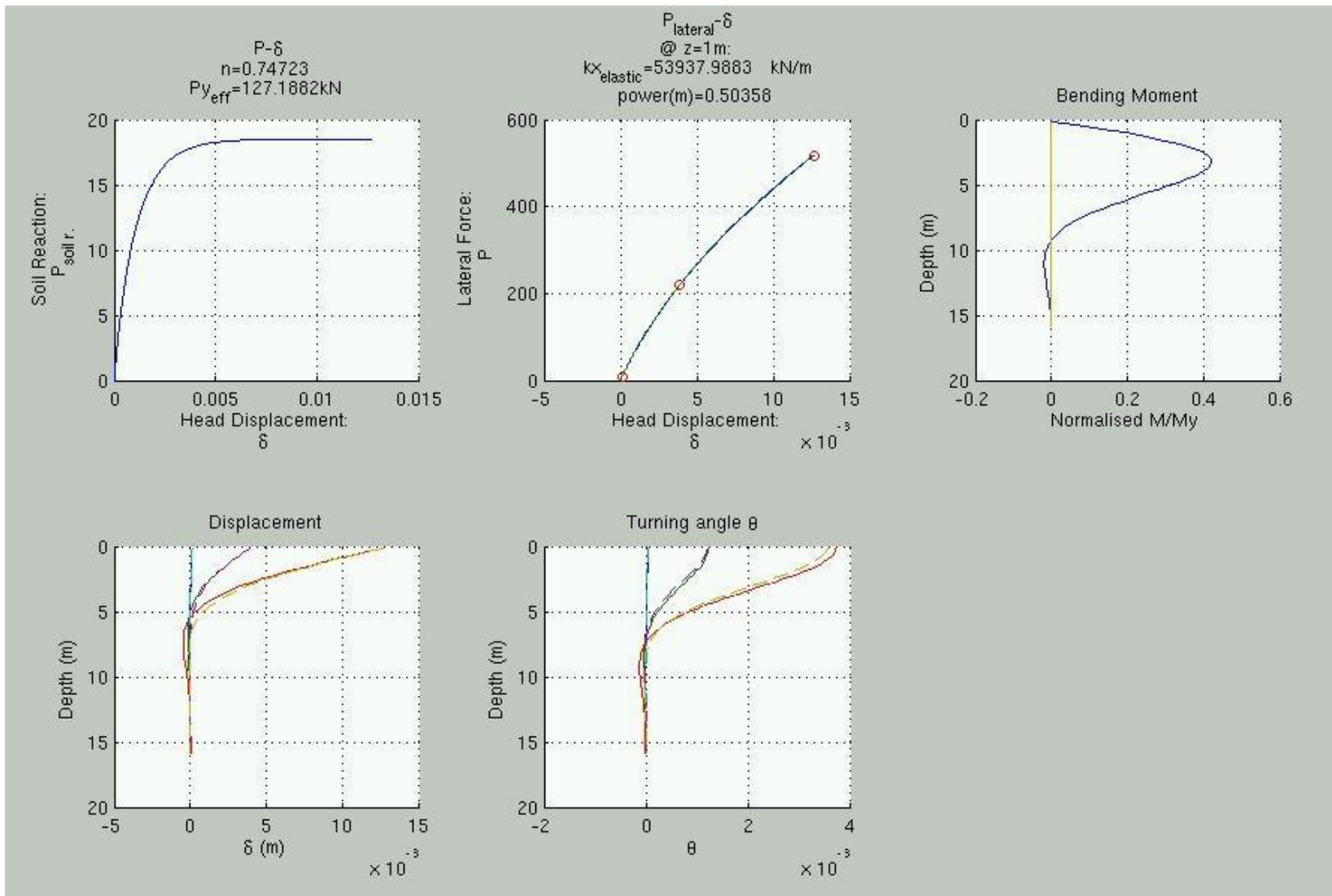


FIGURE 3.2.7: Validation case: optima  $n, P_y, m$



## Chapter 4

# Conclusions

The calculation of soil parameters, required for designing pile foundation under lateral load - and specifically of the soil spring's initial stiffness  $k_o$  and the exponential power  $m$ , that defines the stiffness' distribution with depth, of the parameter  $n$  that governs the sharpness of transition from the linear to nonlinear range during initial loading and of the ultimate soil reaction  $P_{yo}$  - with speed and acceptable geotechnical accuracy, utilizing the respective incremental static in-situ load test, was achieved, within delimitations. The need of further analyses and more cases, is unquestionable, before more conclusions are made.

**Future Work** Working with the same algorithm, more cases, using in-situ archived data or scaled experiments, could be tested, to determine the full range of its capability, as well as its boundaries. Otherwise, the elimination of the assumptions, delimitations and delimitations of this thesis, e.g. (re)designing an inverse algorithm that support multi-layered soil deposit and dynamic and cyclic lateral load, could be a productive study field.



## Appendix A

# Inverse Analysis Algorithm: Matlab Code

The Inverse Analysis Algorithm implemented into MATLAB<sup>®</sup> environment, version 8.0 (Release 2012b). The code consists of three *.m* files: **main1PL.m**, **fun1PL.m**, **fun2PL.m**. The first one, the script file, should be runned. Its execution cause the other two, function, files to be called.

### A.1 Guidance on input format

As far as input is concerned, the following points should be considered:

- Pile's geometry, ultimate Bending Moment ( $M_y$ ) and modulus of Elasticity, are gathering from the graphical dialog box created by prompt commands , see figure 3.1.1 on p.19.
- Pile's recorded responses are gathering in a matrix saved as a *.txt* script (see the **load\_dispPLAXIS.txt**, B.1.1 on p.53). The script's name should be manually written in the functions *.m* files, **fun1PL.m** and **fun2PL.m**, completing the load command of lines 18 and 16, respectively. Matrix format (whereas  $nL$  and  $nR$  are the number of pile's layers and the response's records, respectively) is:

$$\begin{bmatrix} y_{1,1} & y_{1,2} & y_{1,3} & \dots & y_{1,nR} \\ y_{2,1} & y_{2,2} & y_{2,3} & \dots & y_{2,nR} \\ \vdots & \vdots & \vdots & \ddots & \vdots \\ y_{nL,1} & y_{nL,2} & y_{nL,3} & \dots & y_{nL,nR} \end{bmatrix}$$

- Pile's  $p - y$  curve is gathering in a matrix, saved as a *.txt* script, (see the `load_headDispPLAXIS.txt`, B.1.2 on p.54). The script's name should be manually written in the functions *.m* files, `fun1PL.m` and `fun2PL.m`, completing the load command of lines 17 and 15, respectively. Matrix format (whereas  $nR$  is the number of the records, ) is:

$$\begin{bmatrix} P_1 & y_{head,1} \\ P_2 & y_{head,2} \\ \vdots & \vdots \\ P_{nR} & y_{head,nR} \end{bmatrix}$$

- *Default* values are given for the BWGG parameters  $a_s$  and  $a_p$  equal to 1% (see 2.1.3 on p.9) and the number of iterations used in the forward analysis equal to 1000. These values can be altered changing the relative commands of the *m.* functions. Moreover, default initial estimation is equal to  $k_o^{ref} = 100 \text{ MN/m}^2$ ,  $m = 0.5$ ,  $Py = 500 \text{ kN}$  and  $n = 0.5$  , which define the start point for the optimization's functions, and optimization's options are, also, set as: tolerance for accuracy equal to  $\pm 1\%$  and maximum number of function evaluations equal to 5000. These values can be altered changing the relative commands of the `main1PL.m`.

## A.2 Script: main1PL.m

```

1      %%%%%%%%%%%%%%%%%%%%%%%%%%%%%%%%%%%%%%
2      %%          NLPILE , MAIN EDITOR           %%
3      %% Version:1PL {1 soil LAYER (4parameters)} %%
4      %% optimum: ko & x=[n*10,Pyo/100,m*10]      %%
5      %%%%%%%%%%%%%%%%%%%%%%%%%%%%%%%%%%%%%%%
6 clc
7 %% Input: geometry & strength of PILE
8 prompt={'Enter in m, the pile''s Length (e.g.L=16):','...
9 'Enter in m, the pile''s Diameter (e.g.d=1):',...
10 'Enter in kPa the pile''s modulus of Elastisity (e.g.E=25 000
11 000):',...
12 'Enter in kNm, the pile''s yield Moment (e.g.My=2200):'} ;
13 title='NLpile inverse anlaysis: INPUT ';
14 answer=inputdlg(prompt,title);
15 %
16 tic % time is on
17 profile on
18 %
19 L = str2num(answer{1});
20 d= str2num(answer{2});
21 Epp=str2num(answer{3});
22 My=str2num(answer{4});
23 %
24 App=pi()*d^2/4;
25 Ipp=(pi()*d^4)/64;
26 pile=[L;Epp;App;Ipp;My;1];
27 %
28 %% optimization for Ko
29 version=1;
30 [x] = fminsearch(@(x) fun1PL(x,pile),10 );
31 ko=[0,10000*x];
32 %
33 %% optimization for n,py,power
34 % [kx=(depth^power) *Ko]
35 version=2;
36 options=optimset('TolX',0.01, 'MaxFunEvals',5000,'PlotFcns'
37 ,@optimplotx);

```

```
36 [x]= fminsearch(@(x) fun2PL(x,pile,ko,version),[5,5,5],  
    options);  
37 %  
38 %% create graphics  
39 version=3;  
40 f=fun2PL(x,pile,ko,version);  
41 %  
42 %% output in text format on the Command Window  
43 fprintf('\n-----');  
44 fprintf('\n OPTIMIZATION results:');  
45 fprintf('\n The no.%d Soil Material has n = %.2f .',1,x(1)  
    /10);  
46 fprintf('\n The no.%d Soil Material has Pyo = %.f kN.',1,x  
    (2)*100);  
47 fprintf('\n The no.%d Soil Material has ko = %.f KN/m2.',1,  
    ko(2));  
48 fprintf('\n The no.%d Soil Material has power (kx=ko*depth^  
    power) = %.2f.\n\n',1,x(3)/10);  
49 %  
50 toc % time out  
51 profile viewer
```

### A.3 Function: fun1PL.m

```

1  function f=fun1PL(x,pile)
2 %%%%%%
3 %       about fun1PL(x,pile): %
4 % Goal: Compute optimum elastic Ko,ref %
5 %
6 % Input: x=ko*/10000, ko*=initial estimation, %
7 % [pile]=[ L ; Epp ; App ; Ipp ; My ;1], %
8 % as created from main1PL.m , %
9 % and P-y & pile's respnses (.txt) files, %
10 % which 1st respose is elastic %
11 %%%%%%
12
13 %% INPUT
14 %
15 % Load's input : LATERAL load at
16 % the head of the pile
17 load_headDisp=load('load_headDispPLAXIS.txt');
18 load_disp=load('load_dispPLAXIS.txt');
19 NumLayers=size(load_disp,1)-1;
20 ascale=1; % scale factor=ascale
21 P=load_headDisp(:,1);
22 dispHeadField=load_headDisp(:,2);
23 %
24 % Interpolation of P-y values
25 dispHeadField_elastic=dispHeadField(1:2);
26 dispHeadField=interp1([0 1],dispHeadField_elastic
27     ,[0,0.25,0.5,0.75,1]);
28 Pelastic=P(1:2); P=interp1([0 1],Pelastic
29     ,[0,0.25,0.5,0.75,1]);
30 mm=3; %number of points used in analysis
31 Pmax=P(mm); step=Pmax/(mm-1) ;
32 %
33 % Materials' input:
34 materials=[1,      0.5,      0.001,    0,          2,          0
35             2,      0.5,      0.001, 10000*x(1), 1, 100];
36 NumMaterials=size(materials,1);
37 %

```

```

36 % define materials' properties
37 bl=repmat(0.00001,[NumMaterials,1]);mat_n=bl;nl=bl;a=bl;ko=
38     bl;Pyo=bl;power=bl;
39 for i=1:NumMaterials,
40 mat_n(i)=materials(i,1); bl(i)=materials(i,2); a(i)=
41     materials(i,3);
42 nl(i)=materials(i,5); ko(i)=materials(i,4); Pyo(i)=
43     materials(i,6);
44 end
45 %
46 % define x
47 for i=2:NumMaterials,
48     x(i-1)=ko(i)/10000;
49 end
50 %
51 % Pile's input
52 L=pile(1);
53 nL=NumLayers;
54 pile=[L/nL;pile(2:end)]';
55 pile= [(1:nL)',repmat(pile,[nL,1])]; % ( NumLayers x 7)
56 nn=nL+4; % plus 4 pseudo-nodes;
57 %
58 % [Pile]= extended matrix of [pile], (nn x 7)
59 % (IMAGINARY nodes INCLUDED)
60 % {#3=head of pile, #(nn-2)=pinpoint of pile=deeper point},
61 Pile=zeros(nn,size(pile,2));
62 for i=1:2, Pile(i,:)=pile(1,:);
63 end
64 for i=nn-1:nn, Pile(i,:)=pile(nn-4,:);
65 end
66 Pile(3:nn-2,:)=pile;
67 %
68 h=zeros(nn,1); Epp=h; App=h; Ipp=h; My=h;
69 depth=h; lay_matp=ones(nn,1); lay_n=h; wyp=h;
70 for i=1:nn,
71     lay_n(i)=Pile(i,1); h(i)=Pile(i,2); Epp(i)=Pile(i,3);
72     App(i)=Pile(i,4); Ipp(i)=Pile(i,5);
73     My(i)=Pile(i,6); lay_matp(i)=Pile(i,7);
74     wyp(i)=My(i)/(Epp(i)*Ipp(i));depth(i+1)=depth(i)+h(i);

```

```

72 end
73 depth=abs(depth-h(1)-h(2)/2); depth(1)=0.01;
74 EI=Epp.*Ipp;
75 EIo=EI;
76 %
77 % SOIL profile
78 % soil=[layer #,soil material,OCR], (NumLayers x 3)
79 soil=[1:nL;repmat(2,1,nL);ones(1,round(nL/20)),repmat(1,1,nL
    -round(nL/20))]';
80 Soil_Input=size(soil,2);
81 Soil=zeros(nn,Soil_Input);
82 %
83 % [Soil]= extended matrix of [soil]
84 % (IMAGINARY nodes INCLUDED), (nn x 3)
85 for i=1:2, Soil(i,:)=soil(1,:);
86 end
87 for i=nn-1:nn, Soil(i,:)=soil(nn-4,:);
88 end
89 Soil(3:nn-2,:)=soil;
90 %
91 kx=zeros(nn,1);lay_mats=kx; py=kx; % define size
92 for i=1:nn
93 lay_mats(i)=Soil(i,2); OCR=Soil(i,3); ims=lay_mats(i);
94     if OCR ==1,
95         kx(i)=ko(ims)*(depth(i)); %^power(ims), searching
96         only the kref;
97         py(i)=Pyo(ims)*depth(i) ;
98     else    kx(i)=kx(i-1); py(i)=py(i-1); % if OCR>1;
99     end
100 end
101 wys=py./kx;
102 kxo=kx;
103 %
104 % materials properties of each layer
105 bp=zeros(nn,1);bs=bp;gp=bp;gs=bp;
106 np=bp;Ap=bp;As=bp;ap=bp;as=bp;cm=bp;ns=bp;
107 %
108 for i=1:nn
109 im=lay_matp(i); ims=lay_mats(i);

```

```

109 bp(i)=bl(im); bs(i)=bl(ims);
110 gp(i)=1-bl(im); gs(i)=1-bl(ims);
111 np(i)=nl(im); ns(i)=nl(ims);
112 ap(i)=a(im); as(i)=a(ims);
113 end
114 %
115 %% w(node,repetition)=w(i,j): DISPLACEMENTS of each node of
116 % the PILE
117 %
118 w=zeros(nn,mm); curv=w; theta=w; Mom=w;
119 Shear=w; EI_saved=w; kx_saved=w;
120 KK=zeros(nn,nn); F=zeros(nn,1); dw=F;
121 d2EI_saved=w; zetaSaved=w;
122 zetasSaved=w; zetas=F; dzetas=F;
123 zetap=F; dzetap=F; Soil_Reaction=zeros(nn,mm);
124 Ksaved=ones(nn,mm); EI_saved(:,1)=EI; go=1;
125 %
126 for j=1:mm-1
127 % BOUNDARY CONDITIONS
128 % head of pile (node 3), [ Shear=P;Mom=0]
129 dEI=(EI(4)-EI(2))/EI(3);
130 KK(1:2,1:5)=[-1,2+dEI,-2*dEI,-2+dEI,1; 0,1,-2,1,0];
131 %
132 % pinpoint of pile (node nn-2), [ Mom=0;Shear=0]
133 KK(nn-1:nn,nn-4:nn)=[0,1,-2,1,0; -1,2,0,-2,1];
134 %
135 % q= d2(Mom)/dx2= d2(EI* d2w/dx2)/dx2
136 for i=3:nn-2
137 Dx4=h(i)^4;
138 d2EI=( EI(i-1)-2*EI(i)+EI(i+1))/EI(i);
139 Ki= 6 + kx(i)*(Dx4) /EI(i)- 2*d2EI;
140 KK(i,i-2:i+2)=[1 ,-4+d2EI,Ki ,-4+d2EI ,1];
141 Ksaved(i,j+1)=Ki;
142 d2EI_saved(i,j)=d2EI;
143 end
144 %
145 F(1)=ascale*step *2*(h(3)^3)/EI(3); % Shear @ node 3 =
146 % lateral load
147 %

```

```

145 dw=KK\F;
146 w(:, j+1) =w(:, j)+dw;
147 %
148 for n=3:nn-2,
149 theta(n, j+1)=(w(n-1, j)-w(n+1, j))/ 2/(h(n));
150 curv(n, j+1)=(w(n+1, j)-2*w(n, j)+w(n-1, j))/h(n)/h(n);
151 end
152 %
153 % NonLinearity of PILE:
154 dcurv=curv(:, j+1)-curv(:, j);
155 dzetap=(1-(bp+gp.*sign(dcurv.*zetap)).*(abs(zetap)).^np).*dcurv./wyp;
156 zetap=zetap +dzetap;
157 EI=ap.*EIo + ...
158 (1-ap).*EIo.*(1-(bp+gp.*sign(dcurv.*zetap)).*(abs(
159 zetap)).^np);
160 EI_saved(:, j+1)=EI;
161 zetapSaved(:, j+1)=zetap;
162 %
163 % NonLinearity of GROUND:
164 dzetas=(1-(bs+gs.*sign(dw.*zetas)).*(abs(zetas)).^ns).*dw
165 ./wys;
166 zetas=zetas +dzetas;
167 kx=as.*kxo + ...
168 (1-as).*kxo.*(1-(bs+gs.*sign(dw.*zetas)).*(abs(zetas))
169 .^ns);
170 kx_saved(:, j+1)=kx;
171 zetasSaved(:, j+1)=zetas;
172 Soil_Reaction(:, j+1)=zetas.*py.*(1-as) +as.*kxo.* w(:, j+1)
173 ;
174 %
175 % Pile bending MOMENT & SHEAR force
176 Mom(:, j+1)=ap.*EIo.*curv(:, j+1) +(1-ap).*My.*zetap ;
177 for n=3:nn-2, Shear(n, j+1)=Mom(n, j+1)-Mom(n-1, j+1)/h(n)
178 ;
179 end
180 %
181 end
182 %

```

```

178 %
179 %% GRAPHICS
180 %
181 % soil Reaction -displacement @ head of pile
182 figure(1);clf
183 subplot(2,3,1);hold on;grid on;
184 xlabel({'Head Displacement:';'{\delta}'});
185 ylabel({' Soil Reaction:'; ' P_{soil r.} '});
186 plot(w(3,1:mm),Soil_Reaction(3,1:mm))
187 title({' P-{\delta}';['n=',num2str(ns(3))]} )
188 %
189 %Lateral Force- displacement @head of pile
190 subplot(2,3,[2 3]);hold on;grid on;
191 xlabel({; 'Head Displacement:';'{\delta}'});
192 ylabel({' Lateral Force:'; ' P '});
193 plot(w(3,1:mm),P(1:mm),dispHeadField(1:mm),P(1:mm), 'or')
194 title({' P_{lateral}-{\delta}';[];[' k_{eff}= ',num2str(ko(2)
195 , '% .f'), ' kN/m' ]})
196 %
197 % Bending Moment - depth
198 subplot(2,3,4);hold on;grid on;set(gca,'YDir','reverse');
199 plot(Mom(3:nn-2,mm)/My(3:nn-2),depth(3:nn-2));
200 title({'Bending Moment';['P= ',num2str(P(mm),'% .f'), ' kN']})
201 xlabel('Normalised M/My'); ylabel('Depth (m)');
202 % Pile's displacemnt - depth
203 subplot(2,3,5);hold on;grid on;set(gca,'YDir','reverse');
204 plot(w(3:nn-2,mm),depth(3:nn-2));
205 title({'Displacement';['P= ',num2str(P(mm),'% .f'), ' kN']}),
206 xlabel('{\delta (m)}');
207 ylabel('Depth (m)');
208 % Pile's Turning angle- depth
209 subplot(2,3,6);hold on;grid on;set(gca,'YDir','reverse');
210 plot(theta(3:nn-2,mm),depth(3:nn-2));
211 title({'Turning angle {\theta}';['P= ',num2str(P(mm),'% .f')
212 , ' kN']}),
213 xlabel('{\theta}');
214 ylabel('Depth (m)');
215 %
216 %

```

```
215 %% deviation: field vs computed
216 f=0 + (1/sqrt(2)) *norm((w(3,1:2)-dispHeadField(1:2)))
217     +(1/sqrt(2))*norm((w(nL,1:2)-zeros(1,2)));
    end
```

## A.4 Function: fun2PL.m

```

1      function f=fun2PL(x,pile,ko,version)
2 %%%%%%
3 %       about fun2PL(x,pile); %
4 % Goal: Compute optimum elastic Ko,ref %
5 %
6 % Input: x=ko*/10000, ko*=initial estimation, %
7 % [pile]=[ L ; Epp ; App ; Ipp ; My ;1], %
8 % as created from main1PL.m , %
9 % and P-y & pile's respnses (.txt) files, %
10 % which 1st respose is elastic %
11 %%%%%%
12 %
13 %% FIELD VALUES/ INPUT
14 L=pile(1);
15 load_headDisp=load('load_headDispPLAXIS.txt');
16 load_disp=load('load_dispPLAXIS.txt');
17 NumLayers=size(load_disp,1)-1; thickness=L/NumLayers;
18 NumRecords=size(load_disp,2);
19 %
20 % field measured displacements
21 Pfield=load_disp(1,1:NumRecords);
22 dispField=load_disp(2:end,1:NumRecords);
23 dispHeadField=dispField(1,:);
24 thetaField=zeros(NumLayers,NumRecords);
25 for j=1:NumRecords
26 for i=1:NumLayers-1
27     thetaField(i,j)=(dispField(i,j)-dispField(i+1,j))/%
28         thickness;
29 end
30 end
31 %
32 % Interpolation
33 wanted_Num_analysis_points=1000;
34 mm=wanted_Num_analysis_points;
35 load_step=max(Pfield)/(mm-1) ;
36 %
37 Pi=interp1(Pfield,Pfield,0:load_step:max(Pfield),'*cube');

```

```
37 step=load_step;
38 indexField=zeros(NumRecords ,1);
39 %
40 for i=1:NumRecords
41     p=Pfield(i);
42 index=find((abs(Pi-p))<step);
43 indexField(i)=index(1);
44 end
45 dispHeadFieldi=interp1(Pfield,dispHeadField,Pi,'*cube');
46 %
47 %
48 %% materials
49 materials=[1,0.5,0.001
50             2,0.5,0.001];
51 NumMaterials=size(materials,1);
52 nL=NumLayers;
53 nn=nL+4;
54 %
55 % materials' properties
56 bl=repmat(0.00001,[NumMaterials,1]);mat_n=bl;nl=bl;a=bl;Pyo=
57     bl; power=bl;
58 for i=1:NumMaterials,
59     mat_n(i)=materials(i,1); bl(i)=materials(i,2); a(i)=
60         materials(i,3);
61 end
62 %
63 % define x
64 nl(1)=2; % concrete
65 for i=2:NumMaterials,
66     nl(i)=x(i-1)/10;
67     Pyo(i)=x(i-1+NumMaterials-1)*100;
68     power(i)=x(i-1 +2*(NumMaterials-1))/10;
69 end
70 %
71 % Pile
72 pile=[thickness;pile(2:end)]';
73 pile= [(1:NumLayers)',repmat(pile,[NumLayers,1])];
74 %
75 Pile=zeros(nn,size(pile,2));
```

```

74 % [Pile]= extended matrix of [pile] (IMAGINARY nodes
    INCLUDED)
75 % {#3=head of pile, #(nn-2)=pinpoint of pile=deeper point}
76 for i=1:2, Pile(i,:)=pile(1,:);
77 end
78 for i=nn-1:nn, Pile(i,:)=pile(nn-4,:);
79 end
80 Pile(3:nn-2,:)=pile;
81 %
82 h=zeros(nn,1); Epp=h; App=h; Ipp=h; My=h;
83 depth=h; lay_matp=ones(nn,1); lay_n=h; wyp=h;
84 for i=1:nn,
85     lay_n(i)=Pile(i,1); h(i)=Pile(i,2); Epp(i)=Pile(i,3);
86     App(i)=Pile(i,4); Ipp(i)=Pile(i,5);
87     My(i)=Pile(i,6); lay_matp(i)=Pile(i,7);
88     wyp(i)=My(i)/(Epp(i)*Ipp(i)); depth(i+1)=depth(i)+h(i);
89 end
90 depth=abs(depth-(h(1)-h(2))/2); depth(1)=0.01;
91 EI=Epp.*Ipp;
92 EIo=EI;
93 %
94 % SOIL profile
95 % soil=[layer #,soil material, %OCR]
96 soil=[1:nL; repmat(2,1,nL); ones(1,nL)]';
97 Soil_Input=size(soil,2);
98 size(soil,1);
99 Soil=zeros(nn,Soil_Input);
100 % [Soil]= extended matrix of [soil] (IMAGINARY nodes
    INCLUDED)
101 for i=1:2, Soil(i,:)=soil(1,:);
102 end
103 for i=nn-1:nn, Soil(i,:)=soil(nn-4,:);
104 end
105 Soil(3:nn-2,:)=soil;
106 %
107 kx=zeros(nn,1); lay_mats=kx; py=kx; % define size
108 for i=1:nn
109     lay_mats(i)=Soil(i,2);
110     % OCR=Soil(i,3);

```

```

111 ims=lay_mats(i);
112 %           if OCR ==1,
113 kx(i)=ko(ims)*(depth(i))^power(ims);
114 py(i)=Pyo(ims)*depth(i) ;
115 %           else kx(i)=kx(i-1); py(i)=py(i-1); % if OCR>1;
116 %
117 end
118 wys=py./kx;
119 kxo=kx;
120 %
121 % define properties of each node
122 bp=zeros(nn,1); bs=bp; gp=bp; gs=bp;
123 np=bp; ap=bp; as=bp; ns=bp;
124 for i=1:nn
125 im=lay_matp(i); ims=lay_mats(i);
126 bp(i)=bl(im); bs(i)=bl(ims);
127 gp(i)=1-bl(im); gs(i)=1-bl(ims);
128 np(i)=nl(im); ns(i)=nl(ims);
129 ap(i)=a(im); as(i)=a(ims);
130 end
131 %
132 %
133 %% w(node,repetition)=w(i,j): DISPLACEMENTS of each node of
134 % the PILE
135 %
136 w=zeros(nn,mm); curv=w; theta=w; Mom=w; Shear=w; EI_saved=w;
137 kx_saved=w;
138 KK=zeros(nn,nn); F=zeros(nn,1); dw=F; d2EI_saved=w;
139 zetaSaved=w; aa=w;
140 zetasSaved=w; zetas=F; dzetas=F; zetap=F; dzetap=F;
141 Soil_Reaction=zeros(nn,mm);
142 Ksaved=ones(nn,mm); EI_saved(:,1)=EI;
143 %
144 % go=1;
145 %
146 for j=1:mm-1
147 %
148 % BOUNDARY CONDITIONS
149 % head of pile (node 3), [ Shear=P;Mom=0]
150 dEI=(EI(4)-EI(2))/EI(3);

```

```

146    KK(1:2,1:5)=[-1,2+dEI,-2*dEI,-2+dEI,1; 0,1,-2,1,0];
147    % pinpoint of pile (node nn-2), [ Mom=0;Shear=0]
148    KK(nn-1:nn,nn-4:nn)=[0,1,-2,1,0; -1,2,0,-2,1];
149    %
150    % q= d2(Mom)/dx2= d2(EI* d2w/dx2)/dx2
151    for i=3:nn-2
152        Dx4=h(i)^4;
153        d2EI=( EI(i-1)-2*EI(i)+EI(i+1))/EI(i);
154        Ki= 6 + kx(i)*(Dx4) /EI(i)- 2*d2EI;
155        KK(i,i-2:i+2)=[1,-4+d2EI,Ki,-4+d2EI,1];
156        Ksaved(i,j+1)=Ki;
157        d2EIsaved(i,j)=d2EI;
158    end
159    %
160    % Shear @ node 3 = lateral load
161    F(1)=step *2*(h(3)^3)/EI(3);
162    %
163    dw=KK\F;
164    w(:,j+1) =w(:,j)+dw;
165    %
166    for n=3:nn-2,
167        theta(n,j+1)=(w(n-1,j)-w(n+1,j))/ 2/(h(n));
168        curv(n,j+1)= (w(n+1,j)-2*w(n,j)+w(n-1,j)) /h(n)/h(n);
169    end
170    %
171    %
172    % NonLinearity of PILE:
173    dcurv=curv(:,j+1)-curv(:,j);
174    dzetap=(1-(bp+gp.*sign(dcurv.*zetap))).*(abs(zetap)).^np).*dcurv./wyp;
175    zetap=zetap +dzetap;
176    EI=ap.*EIo + ...
177        (1-ap).*EIo.*(1-(bp+gp.*sign(dcurv.*zetap))).*(abs(
178            zetap)).^np);
179    EIsaved(:,j+1)=EI;
180    zetapSaved(:,j+1)=zetap;
181    %
182    % NonLinearity of GROUND:

```

```

182 dzetas=(1-(bs+gs.*sign(dw.*zetas)).*(abs(zetas)).^ns).*dw
183 ./wys;
184 zetas=zetas +dzetas;
185 kx=as.*kxo +...
186 (1-as).*kxo.*(1-(bs+gs.*sign(dw.*zetas)).*(abs(zetas)).^ns
187 );
188 kxsaved(:,j+1)=kx;
189 zetasSaved(:,j+1)=zetas;
190 Soil_Reaction(:,j+1)=zetas.*py.*(1-as) +as.*kxo.* w(:,j+1)
191 ;
192 %
193 % Pile bending MOMENT & SHEAR force
194 Mom(:,j+1)=ap.*EIo.*curv(:,j+1)+(1-ap).*My.*zetap ;
195 for n=3:nn-2, Shear(n,j+1)=Mom(n,j+1)-Mom(n-1,j+1)/h(n)
196 ;
197 end
198 end
199 %
200 %
201 %% GRAPHICS
202 %
203 if version ==3,
204 fprintf('\n-----');
205 fprintf('\n INPUT evaluaton:');
206 fprintf('\n %.1f m is the length of the pile.',L);
207 fprintf('\n %.3g m is the average thickness of layers.',L/(
208 NumLayers));
209 fprintf('\n %d materials have been read.',NumMaterials);
210 fprintf('\n %d layers have been read.',NumLayers);
211 fprintf('\n %.1f kN have been laterally loaded (head of
212 pile).',max(Pfield));
213 fprintf('\n %.2f kN is the used load-step.\n',step);
214 end
215 %
216 % Soil Reaction- displacement @head of pile
217 figure(2);clf
218 subplot(2,3,1);hold on;grid on;
219 xlabel({' Head Displacement:';'{\delta (m)}'});
220 ylabel({' Soil Reaction:'; ' P_{soil} (kN)'});

```

```

215 plot(w(3,1:mm),Soil_Reaction(3,1:mm))
216 title({' P_{soil}- {\delta}' ;...
217     ['n=' ,num2str(ns(3),'% .2f')];...
218     ['P_{eff}=' ,num2str(Pyo(2),'% .f'), 'kN']]})
219 %
220 % Lateral Force- displacement @head of pile
221 subplot(2,3,[2 3]);hold on;grid on;
222 xlabel({';Head Displacement {\delta (m)} :'});
223 ylabel({' Lateral Force (P, kN):'});
224 plot(w(3,1:mm),Pi,dispHeadFieldi,Pi,'--r',dispHeadField,
      Pfield,'or');
225 title({' P_{lateral}-{\delta}' ;...
226     [' kx_{elastic}=' ,num2str(ko(2),'% .f'), ' kN/m' ...
227     , ' ', 'power(m)= ' ,num2str(power(2),'% .2f')];})
228 %
229 % Bending Moment - depth
230 subplot(2,3,4);hold on;grid on;set(gca,'YDir','reverse');
231 plot(Mom(3:nn-2,mm)/My(3:nn-2),depth(3:nn-2));
232 title({'Bending Moment';['P=' ,num2str(Pi(mm),'% .f'), ' kN'...
    ]}),
233 xlabel('Normalised M/My');ylabel('Depth (m)');
234 %
235 % Pile's displacement -depth
236 subplot(2,3,5);hold on;grid on;set(gca,'YDir','reverse');
237 plot(w(3:nn-2,indexField),depth(3:nn-2),'b',dispField,depth
      (3:nn-2),'-.r');
238 title('Displacement'),
239 xlabel('{\delta (m)}');
240 ylabel('Depth (m)');
241 %
242 % Pile's Turning angle -depth
243 subplot(2,3,6);hold on;grid on;set(gca,'YDir','reverse');
244 plot(theta(3:nn-2,indexField),depth(3:nn-2),'b',thetaField,
      depth(3:nn-2),'-.r');
245 title('Turning angle {\theta }'),
246 xlabel('{\theta }');
247 ylabel('Depth (m)');
248 %
249 %

```

```
250 %% deviation: field VS computed arguments
251 h=0;g=0;h1=0;
252 for i=1:max(size(x))
253     if x(i)<0, h=1000;
254     end
255 end
256 %
257 for i=1:NumRecords
258 m=indexField(i);
259 %
260 h=h +(1/sqrt(NumLayers))*norm(w(3:nn-2,m)-dispField(:,i)) +
261     (1/sqrt(NumLayers))*(max(dispField(:,i))/max(thetaField
262     (:,i)))*norm(theta(3:nn-2,m)-thetaField(:,i));
263 %
264 g=g+norm((w(3,m)-dispHeadField(i)))/sqrt(NumRecords);
265 end
266 f=(h+g+h1);
267 %
268 end
```



## Appendix B

# Finite Elements 3D analysis

Finite Elements Method (FEM) software, PLAXIS 3D<sup>©</sup> was used in order to produce single pile response to lateral load, so as to validate the developed algorithm.

In this chapter results of this analysis are presented. First, in the format compatible with the MATLAB code of the inverse analysis, afterwards, in the report PLAXIS produce to synthesize the main output and, also, the materials used. Finally, additional figures created from FEM analysis are placed in the last subsection.

### B.1 Input used in Validation Case

Results of 3D FEM analysis are presented in the format compatible with the MATLAB code of the inverse analysis, as explained in the ch.A.1 on p.33. Important is that the first load should be small enough not to provoke inelastic response of the pile.

#### B.1.1 P-y curve

load\_headDispPLAXIS.txt

---

10	0.000117642
220	0.0037269628
518	0.0121313528

---

### B.1.2 Displacement's distribution

load\_dispPLAXIS.txt

10	220	518
0.0001233553	0.003904409	0.0126515678
0.0001119286	0.0035495166	0.0116111378
0.0001007172	0.0031993882	0.0105815264
0.000089901	0.0028585867	0.0095732079
7.9611296030022E-005	0.0025310845	0.0085954683
6.99554282879493E-005	0.0022205082	0.0076569439
0.000060991	0.0019293405	0.0067639509
0.000052767	0.0016599251	0.0059227423
4.52947748674577E-005	0.00141349	0.0051374713
3.8577718755863E-005	0.0011909963	0.0044120448
3.25948405679969E-005	0.0009924292	0.003748595
2.7319176014695E-005	0.0008174579	0.0031486457
2.27097401427826E-005	0.0006650313	0.0026119682
1.87205242860784E-005	0.0005338173	0.0021374554
1.5303205311975E-005	0.0004222683	0.0017228194
1.24010644665075E-005	0.0003284809	0.0013647077
0.000009966	0.0002508106	0.0010600055
7.94040804856772E-006	0.0001872308	0.000803847
6.27689693926466E-006	0.0001360572	0.0005920808
4.92612459566748E-006	9.55317277760663E-005	0.000419645
3.8435931299679E-006	6.40662721584517E-005	0.0002817381
2.98839323854935E-006	4.02033727836609E-005	0.0001735792
2.32272290301809E-006	0.000022598	9.06437749256691E-005
1.81649274816065E-006	0.000010184	2.91855265504849E-005
1.43749644193348E-006	0.000001825	-1.4871294821593E-005
0.000001163	-3.272593769223E-006	-4.4501711314042E-005
9.69130888929538E-007	-5.93948636195215E-006	-6.28702567418048E-005
8.39617208808309E-007	-6.73278727919543E-006	-7.2192407521437E-005
7.57752894190005E-007	-6.22016798294316E-006	-7.4767330582904E-005
0.000000711	-4.81834061286833E-006	-7.23668439612574E-005
0.000000689	-0.000002867	-6.64709049072734E-005
6.83288120245687E-007	-6.33825662805782E-007	-5.83123804536071E-005
6.876570281985E-007	1.68641373429192E-006	-4.88142853786525E-005
0.000000697	3.9427453498096E-006	-3.87527046281134E-005
7.07344719993175E-007	6.02494348217307E-006	-0.000028724
7.16158089768108E-007	7.8663615775678E-006	-1.91444464426885E-005
7.21545961930317E-007	9.42517289651543E-006	-1.03177342723633E-005
7.222519944024101E-007	1.06885099403724E-005	-2.4123577864859E-006
7.18292382890172E-007	1.16488608812464E-005	4.43328055172048E-006
7.08920210971597E-007	0.000012325	0.000010215
6.94344648486205E-007	1.2731284294993E-005	1.49107005587346E-005
6.75091876628355E-007	1.28978427155829E-005	1.85974519693464E-005
6.51609755724687E-007	1.28532154386249E-005	2.13373354550553E-005

---

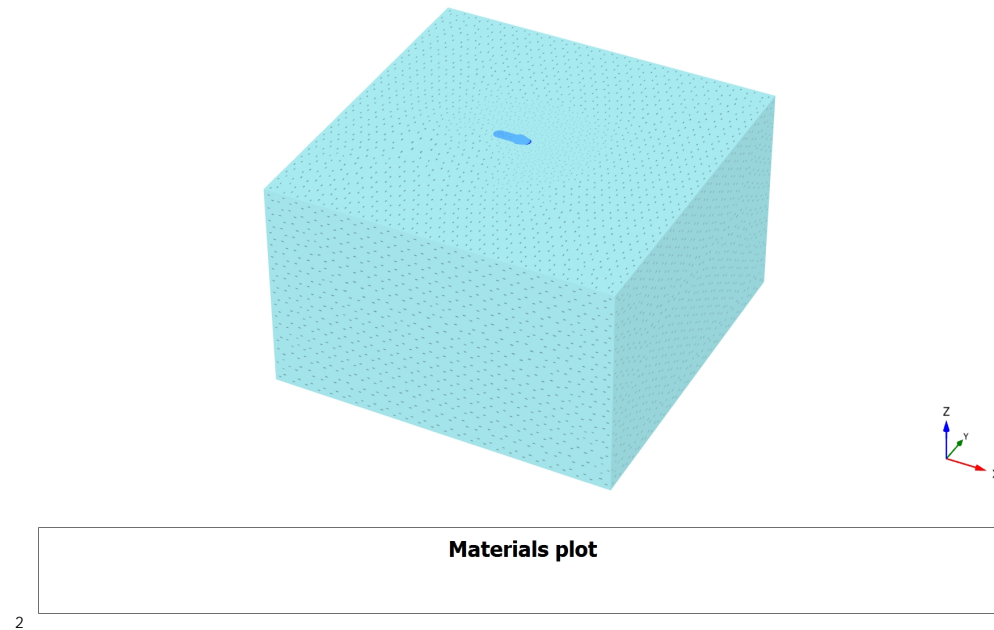
6.24537929426426E-007	0.000012628	2.32304918680934E-005
5.94549010448835E-007	1.2254319469929E-005	2.43838203413711E-005
5.62283771171139E-007	1.17606834551304E-005	2.49042894985048E-005
5.2838790607046E-007	0.000011175	2.49042975018907E-005
4.93412157218338E-007	0.000010521	2.44830614202188E-005
4.5784259751531E-007	9.8196087770393E-006	2.37357501100346E-005
4.22076852928449E-007	9.08851703357214E-006	2.27446573690005E-005
3.86425543243916E-007	8.34218448226832E-006	2.15853614784232E-005
3.51113130212172E-007	7.59157613457067E-006	2.03186880722826E-005
3.16265026685966E-007	0.000006845	1.90016539485918E-005
0.000000282	6.10792991314019E-006	1.76720945326672E-005
2.48062553195737E-007	5.38175728706447E-006	1.63786631018271E-005

---

## **B.2 PLAXIS Report**

The report, that PLAXIS produce to synopsize the main output and the materials used, follows in the next page.

## 1.1.1.1 Calculation results, Phase\_3 [Phase\_3] (3/24), Materials plot



### 1.1.2.1.1 Materials - Soil and interfaces - Hardening soil

Identification	soil
Identification number	1
Drainage type	Drained
Colour	
Comments	
unsat	kN/m <sup>3</sup>
sat	kN/m <sup>3</sup>
Dilatancy cut-off	No
e <sub>init</sub>	0.5000
e <sub>min</sub>	0.000
e <sub>max</sub>	999.0
Rayleigh	0.000
Rayleigh	0.000
E <sub>50</sub> <sup>ref</sup>	kN/m <sup>2</sup>
E <sub>oed</sub> <sup>ref</sup>	kN/m <sup>2</sup>
E <sub>ur</sub> <sup>ref</sup>	kN/m <sup>2</sup>
power (m)	0.5000

Identification		soil
Use alternatives		No
$C_c$		6.900E-3
$C_s$		2.070E-3
$e_{init}$		0.5000
$C_{ref}$	kN/m <sup>2</sup>	0.1000
(phi)	°	32.00
(psi)	°	0.000
Set to default values		No
$ur$		0.2000
$p_{ref}$	kN/m <sup>2</sup>	100.0
$K_0^{nc}$		0.4701
$C_{inc}$	kN/m <sup>2</sup> /m	0.000
$Z_{ref}$	m	0.000
$R_f$		0.9000
Tension cut-off		No
Tensile strength	kN/m <sup>2</sup>	10.00E6
Strength		Rigid
$R_{inter}$		1.000
inter		0.000

Identification	soil
K <sub>o</sub> determination	Automatic
K <sub>0,x</sub> = K <sub>0,y</sub>	Yes
K <sub>0,x</sub>	0.4701
K <sub>0,y</sub>	0.4701
OCR	1.000
POP	kN/m <sup>2</sup>
k <sub>x</sub>	m/s
k <sub>y</sub>	m/s
k <sub>z</sub>	m/s
e <sub>init</sub>	0.5000
c <sub>k</sub>	1.000E15

### 1.1.2.1.2 Materials - Soil and interfaces - Mohr-Coulomb

Identification	RC
Identification number	2
Drainage type	Drained
Colour	
Comments	
unsat	kN/m <sup>3</sup>
sat	kN/m <sup>3</sup>
Dilatancy cut-off	No
e <sub>init</sub>	0.5000
e <sub>min</sub>	0.000
e <sub>max</sub>	999.0
Rayleigh	0.000
Rayleigh	0.000
E	kN/m <sup>2</sup>
(nu)	0.2000
G	kN/m <sup>2</sup>
E <sub>oed</sub>	kN/m <sup>2</sup>

Identification		RC
$C_{ref}$	kN/m <sup>2</sup>	15.26E3
(phi)	°	0.000
(psi)	°	0.000
$V_s$	m/s	2259
$V_p$	m/s	3689
Set to default values		No
$E_{inc}$	kN/m <sup>2</sup> /m	0.000
$Z_{ref}$	m	0.000
$C_{inc}$	kN/m <sup>2</sup> /m	0.000
$Z_{ref}$	m	0.000
Tension cut-off		Yes
Tensile strength	kN/m <sup>2</sup>	7534
Strength		Rigid
$R_{inter}$		1.000
inter		0.000
$K_0$ determination		Automatic
$K_{0,x} = K_{0,y}$		Yes
$K_{0,x}$		1.000
$K_{0,y}$		1.000

ZOLOTA-PILE-LOAD-TEST

Identification	RC
$k_x$	m/s 0.000
$k_y$	m/s 0.000
$k_z$	m/s 0.000
$e_{init}$	0.5000
$c_k$	1.000E15

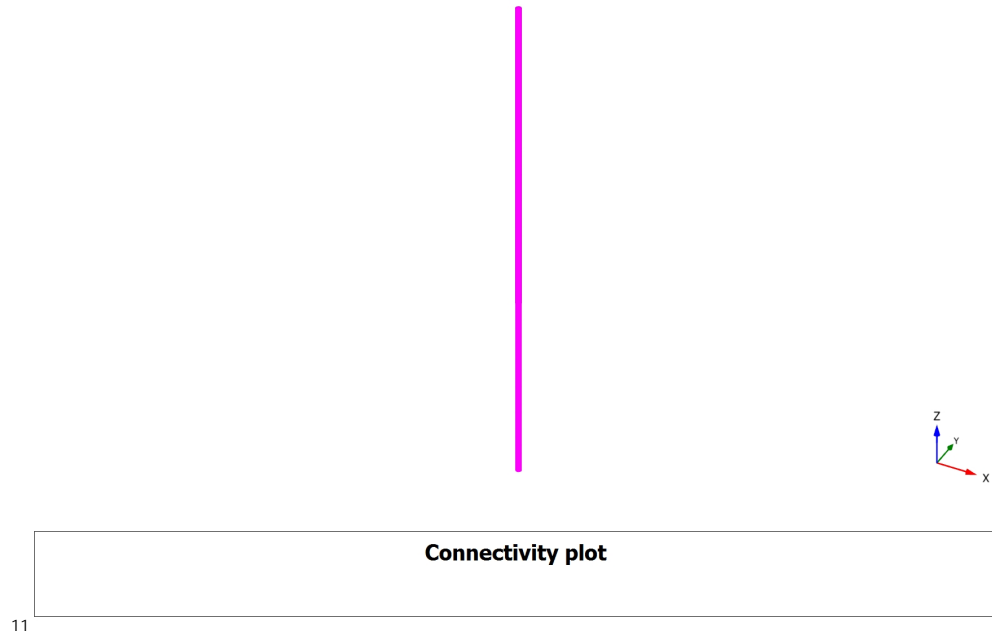
### 1.1.2.2 Materials - Plates -

Identification		head
Identification number		1
Comments		
Colour		
d	m	10.00
	kN/m <sup>3</sup>	0.1000E-3
Linear		Yes
Isotropic		Yes
E <sub>1</sub>	kN/m <sup>2</sup>	25.00E6
E <sub>2</sub>	kN/m <sup>2</sup>	25.00E6
<sub>12</sub>		0.2000
G <sub>12</sub>	kN/m <sup>2</sup>	10.42E6
G <sub>13</sub>	kN/m <sup>2</sup>	10.42E6
G <sub>23</sub>	kN/m <sup>2</sup>	10.42E6
Rayleigh		0.000
Rayleigh		0.000

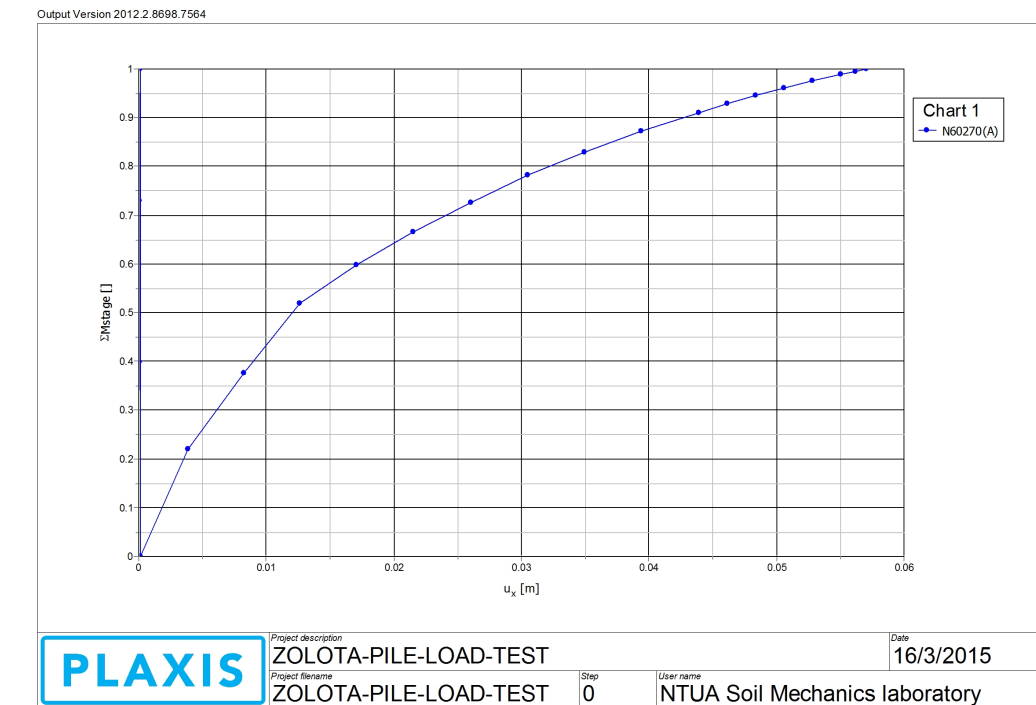
### 1.1.2.3 Materials - Beams -

Identification		inclinometer
Identification number		1
Comments		
Colour		
A	$m^2$	0.7850
	$kN/m^3$	0.1000E-3
Linear		Yes
E	$kN/m^2$	2500
$I_3$	$m^4$	0.04908
$I_2$	$m^4$	0.04908
Rayleigh		0.000
Rayleigh		0.000

## 3.1.1.1.1 Calculation results, Beam, Phase\_3 [Phase\_3] (3/24), Connectivity plot



## 5.1 Chart 1



12

## 5.1.1 Chart 1(N60270(A))

Point	Step	$u_x [10^{-3} \text{ m}]$	Mstage []
0	0	0.000	0.000
1	1	0.000	0.000
2	1	0.000	0.354
3	2	0.000	0.599
4	3	0.000	0.888
5	4	0.000	1.000
6	5	0.000	0.000
7	5	0.042	0.399
8	6	0.084	0.729
9	7	0.123	1.000
10	8	0.123	0.000
11	8	3.904	0.220
12	9	8.277	0.376
13	10	12.652	0.518
14	11	17.098	0.598
15	12	21.557	0.665

ZOLOTA-PILE-LOAD-TEST

Point	Step	$u_x [10^{-3} \text{ m}]$	Mstage []
16	13	26.019	0.726
17	14	30.484	0.781
18	15	34.953	0.829
19	16	39.423	0.872
20	17	43.893	0.910
21	18	46.128	0.928
22	19	48.363	0.945
23	20	50.598	0.960
24	21	52.834	0.975
25	22	55.069	0.988
26	23	56.186	0.995
27	24	57.085	1.000

### B.3 Additional output figures

Figures representing results of the 3D FEM analysis, when the lateral load was ultimate ( $\Sigma M_{stage} = 1$ ).

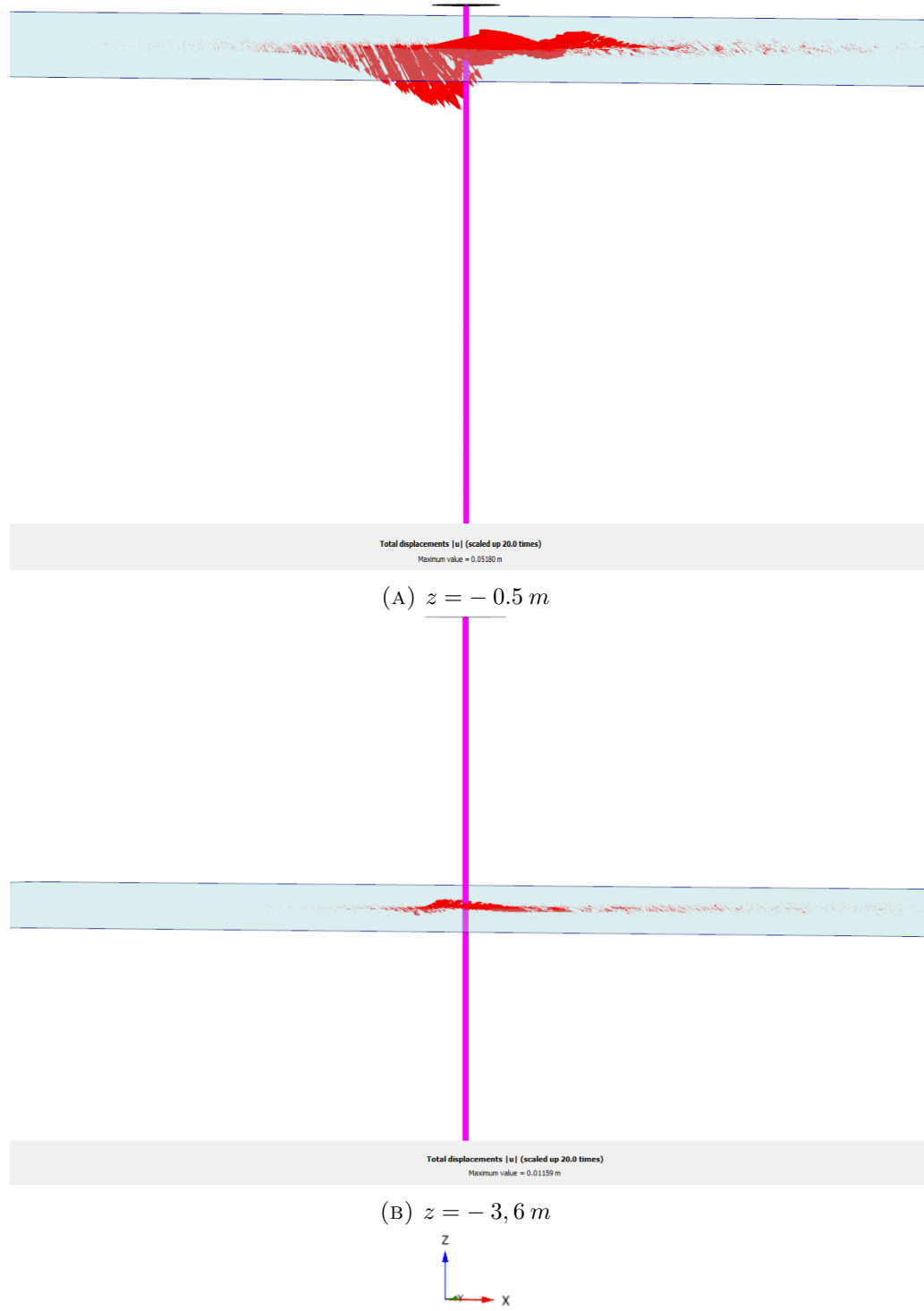
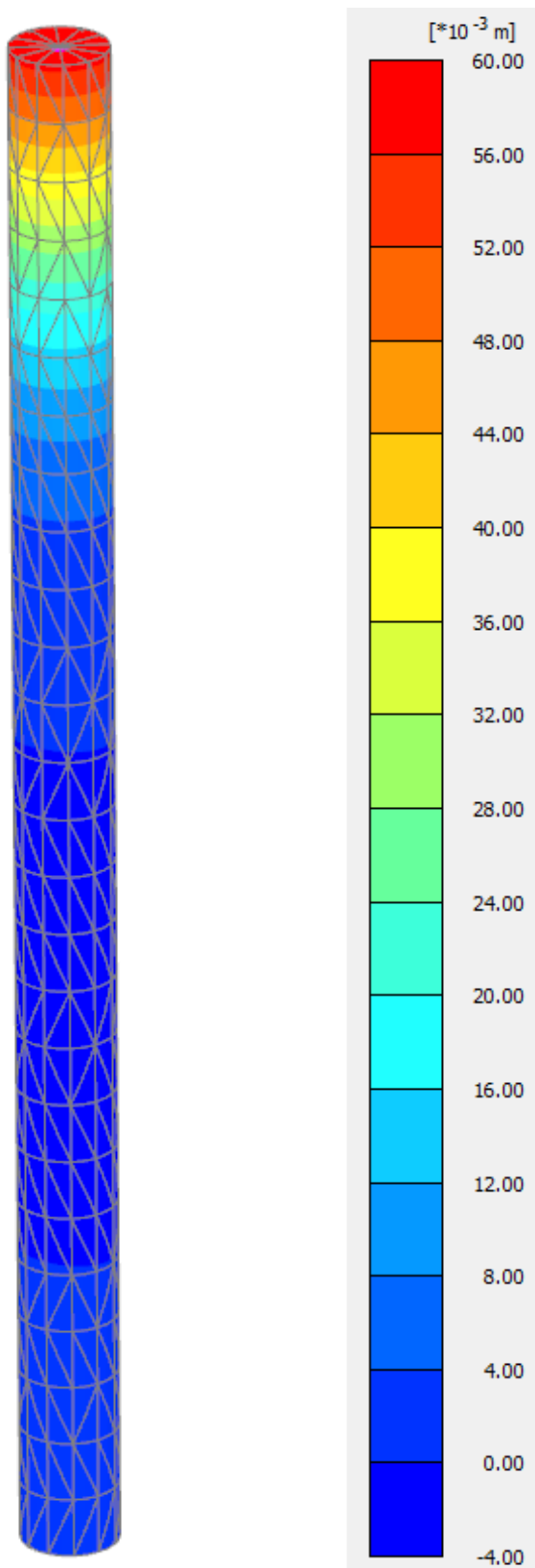
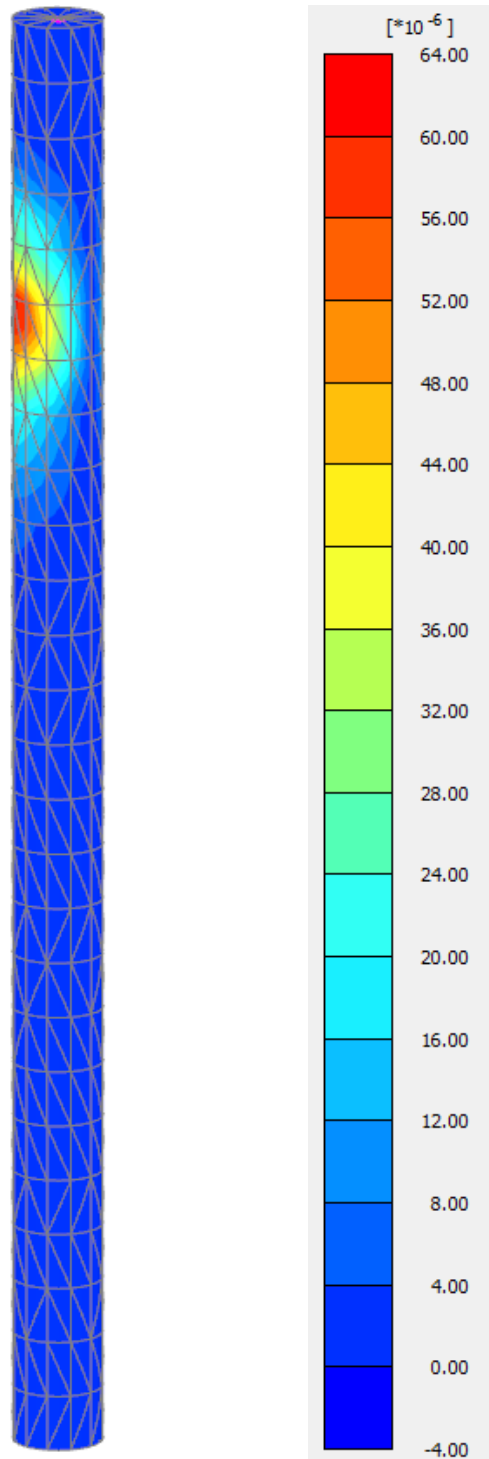


FIGURE B.3.1: Total Displacements,  $u$



---

FIGURE B.3.2: Displacement  $u_x$

**Incremental deviatoric strain  $\Delta\gamma_s$** 

Maximum value =  $0.06080 \times 10^{-3}$  (Element 73451 at Node 40282)

Minimum value =  $0.01055 \times 10^{-6}$  (Element 72985 at Node 69476)

FIGURE B.3.3: Incremental deviatoric strain  $\Delta\gamma_s$



# Bibliography

- [1] N.Gerolymos and G.Gazetas. “phenomenological model applied to inelastic response of soil-pile interaction systems”. *Japanese Geotechnical Society*, 45(4):119–132, August 2005.
- [2] N.Gerolymos et al. “numerical modeling of centrifuge cyclic lateral pile load experiments”. *Earthquake Engineering and Engineering vibration*, 8(1):61–76, March 2009.
- [3] N.Gerolymos. “*Constitutive model for static and dynamic response of soil, soil-pile and soil-caisson*”. PhD thesis, National Technical University of Athens, 2002.
- [4] S.Giannakos. “*Contribution to the Static and Dynamic Lateral Response of Piles*”. PhD thesis, National Technical University of Athens, 2013.
- [5] G.Bouckovalas and N.Gerolymos. “*Computational Geotechnics*”. National Technical University of Athens, 2009. URL <http://users.ntua.gr/gerolymo/COMPUTATIONAL-GEOTECHNICS-BOOK.pdf>. Accessed: 2015-03-10.
- [6] M.Pando, C.Ealy, G.Filz, J.Lesko, and E.Hoppe. “A Laboratory and Field Study of Composite Piles for Bridge Substructures”. Technical report, Federal Highway Administration (FHWA), U.S.Department of Transport, March 2006. URL <http://www.fhwa.dot.gov/publications/research/infrastructure/structures/04043/08.cfm#toc129146966>. Accessed: 2015-03-10.
- [7] A.Anagnostopoulos and B.Papadopoulos. “*Pile Foundations*”. Symeon, Athens, 2004.
- [8] “Optimizing Nonlinear Functions, matlab® documentation”. <http://www.mathworks.com/help/matlab/math/optimizing-nonlinear-functions.html#bsgpq6p-11>, . Accessed: 2015-03-10.
- [9] “Fminsearch, matlab® documentation”. <http://www.mathworks.com/help/matlab/ref/fminsearch.html>, . Accessed: 2015-03-10.

- [10] P.Venkataraman. “*Applied Optimizaton with MATLAB® Programming*”. Wiley-Interscience, New York, 2002.
- [11] N.Gerolymos and G.Gazetas. “lateral response of pile with material and interface nonlinearities.part a:analysis”. In *Proc. 3rd National Conference on Earthquake Engineering and Technical Seismology*, Athens, 2008. URL [http://library.tee.gr/digital/m2368/m2368\\_gerolimos3.pdf](http://library.tee.gr/digital/m2368/m2368_gerolimos3.pdf). Accessed: 2015-03-10.
- [12] T.Schanz et al. “the hardening soil model: Formulation and verification”. In *Proc. Beyond 2000 in Computational Geotechnics – 10 Years of PLAXIS®*, Rotterdam, 1999. URL <http://kb.plaxis.nl/sites/kb.plaxis.nl/files/kb-publications/TheHardeningSoilModel-FormulationandVerfication.pdf>. Accessed: 2015-03-10.
- [13] O.Papakyriakopoulos. “macroelement modeling of the non-lineal response of piles and pile-groups subjected to combined lateral and axial loading”. Diploma thesis, National Technical University of Athens, July 2013.
- [14] Bengt B. Broms. “lateral resistance of piles in cohesionless soils”. *Journal of the Soil Mechanics and Foundations Division*, 90(3):123–158, 1964.
- [15] F.Georges. “development of a computer program for pile and deep foundation analysis in cohesive and cohesionless soils ”. Bachelor thesis, University of Technology, Sydney, November 2014.
- [16] Joseph E.Bowles. “*Foundation analysis and design*”. The McGraw-Hill Companies, Inc., 5th edition.